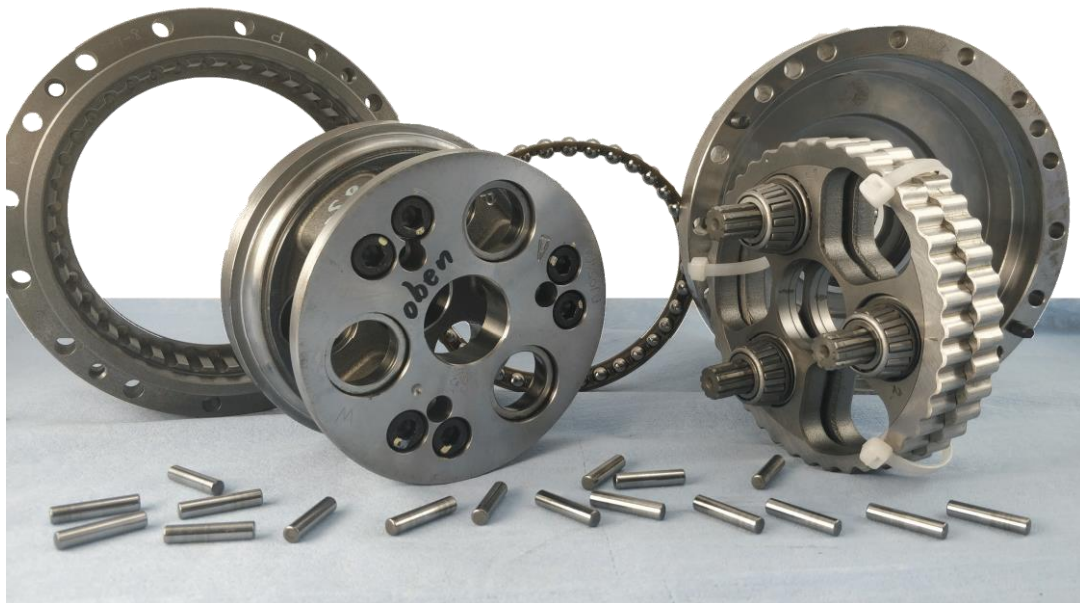


Politecnico di Torino
Corso di Laurea Magistrale in
Ingegneria Meccatronica

Tesi di Laurea Magistrale
Condition Based Monitoring on
Robotic Gearbox



Relatori:

Prof. Giuseppe Quaglia

Dr. Laura Montagna

Dr. Ingo Schulz

Candidato:

Mohamad Amin Al Hajj

“Failure is the opportunity to begin again more intelligently.” – Henry Ford

Abstract

In today's world, robots are becoming more and more influential. Health care, agriculture, food preparation, manufacturing and military are industries with utilization and demand of robots to boost efficiency and convenience for customer and provider.

Although the demand and presence are high, the maintenance of these robots are still preventive rather than predictive. It is challenging to achieve the latter especially in the manufacturing world where the robots' movement include high speed variations. In the market, the maintenance of the robots is done with manners utilizing statistical parameters or specific preprogrammed movements to detect if a damage is present. This needs to be handled in order to move to the predictive maintenance where the down time is only done when it is needed making it less costly and more efficient.

When rotating equipment is involved, Condition Based Monitoring is an established way of getting these data, to analyze and build decisions on them. In this master thesis, the application of different sensors and analysis technologies for automatization and robotics shall be investigated. This research work aims to have an initial step to infer on the state of the robots and specifically the gearboxes inside. The methods of monitoring are vast, but this work uses vibration signals where different sensor implementations shall be tested. Vibration measurements were made on high precision gearboxes with and without defects. Analysis of the data with various techniques is done in addition to an SKF developed algorithm. After which Machine Learning, specifically anomaly detection, is attempted to prove its viability in this task.

The gearboxes used in robots are complicated but intriguing, different implementations have and are used to achieve the requirement of the industry. In this work, the gearbox being tested is the Nabtesco RV-42N, a 2-stage hypocycloidal gearbox, mostly used for robots with 20Kg payload.

Acknowledgements

First, I would like to thank SKF for this opportunity to perform this work, it has been a great learning experience.

Great thanks to Dr. Ingo Schulz, whose support and assistance has been crucial throughout.

Mrs. Laura Montagna, whose perseverance has led to the work being done.

Prof. Giuseppe Quaglia, thank you for all your assistance before and during this task, and for keeping me on track.

I would like to thank the team in Schweinfurt, Martin and Daniel, thank you.

The testing team, I am grateful for your hospitality during the stay in Schweinfurt, helping me feel like home.

The Condition Monitoring experts in SKF, your experience and support has made this achievement possible.

SKF's mechanical department in Airasca, whose companionship during the initial stages has made this work conceivable.

I would like to thank everyone that helped in this work, apologies for not naming each member, but you know that I am grateful for all your support throughout.

To my family, thank you for being there for me, always!

Contents

1.	Introduction	12
2.	Theory	13
2.1	Industry 4.0.....	13
2.2	SKF and Rotating Equipment Performance (REP).....	14
2.2.1	Vision and Strategy	14
2.2.2	Implementation	15
2.3	Robotics	15
2.3.1	Types of robots.....	16
2.3.2	Articulated Robot.....	16
2.4	Gearboxes	17
2.4.1	Robotic Gearboxes.....	17
2.4.2	Nabtesco RV 42-N	18
2.5	Bearings	19
2.5.1	ACBB	19
2.5.2	CRB	20
2.5.3	TRB.....	20
2.6	Sensors	22
2.6.1	Vibration Sensor	22
2.6.2	Temperature Sensor	23
2.6.3	Velocity Sensor.....	23
2.7	State of the Art	24
2.7.1	Previous work	24
2.7.2	Condition Based Monitoring	24
2.7.3	Signal Analysis and Processing	24
2.7.4	Oil Analysis	30
2.7.5	Machine Learning in Vibration Monitoring.....	31
3.	Definition	32
3.1	Target.....	32

3.2	Workflow.....	32
4.	Test Rig.....	33
4.1	Test Rig Setup.....	33
4.2	Noise Cancellation	35
4.3	Robotic Test Cycle	36
4.4	Measurements' Parameters Setup	37
5.	Analysis	40
5.1	Gearbox Kinematics.....	40
5.2	Fundamental Frequencies	42
5.2.1	Gears' Frequencies	42
5.2.2	Bearing Defect Frequencies.....	45
5.3	Results	49
5.3.1	Initial Results	49
5.3.2	Results to mention.....	51
5.4	Dismantled Gearbox	53
5.5	Artificial Defects.....	54
5.5.1	Pinion Wear	54
5.5.2	ACBB, CRB and Disk Damage	55
5.5.3	Interpretation	58
5.6	Machine Learning - PCA.....	59
5.6.1	Implementation	59
5.6.2	Interpretation	60
5.6.3	Conclusion.....	62
6.	Conclusion	63
7.	Future Work.....	64
7.1	Test setup improvements.....	64
7.2	Other Methods.....	64
7.2.1	Defect Detection Methods.....	65
7.2.2	Signal Processing techniques	65
7.2.3	ML.....	66

8.	Bibliography	67
9.	Appendix	70

List of Tables and Figures

Table 1 Accelerometers' Sensitivity and Frequency Range relation [17]	22
Table 2 Test Rig Elements	33
Table 3 Accelerometers and Tachometer used	35
Table 4 Noise Isolation Mats	36
Table 5 Measurements' parameters – Constant Speed	38
Table 6 OT Measurements' parameters – Constant Speed	38
Table 7 Measurements' parameters - Robot Cycle	38
Table 8 OT Measurements parameters - Robot Cycle	38
Table 9 Nabtesco RV-42N parameters [42]	40
Table 10 Gear Ratios [42]	41
Table 11 Fundamental Frequencies of Gears	45
Table 12 Bearings' variables for defect frequency calculations	46
Table 13 Rotation Frequencies of cage and rolling element [48]	46
Table 14 Repetition Frequency of Defect Location [48]	46
Table 15 ACBB variables for defect frequency calculation	46
Table 16 Rotation and Repetition frequencies for ACBB components	47
Table 17 CRB variables for defect frequency calculation	47
Table 18 Rotation and Repetition frequencies for CRB components	47
Table 19 TRB variables for defect frequency calculation	47
Table 20 Rotation and Repetition frequencies for TRB components	48
Table 21 Frequency response to artificial Damages to Gearbox	55
Table 22 Test setup Improvements	64
Figure 1 Life Cycle of a machine (analog.com 2019)	12
Figure 2 From Industry 1.0 to 4.0 (baimatech.com 2018)	13
Figure 3 Rotating Equipment Performance	14
Figure 4 Condition Monitoring system in Sweden [5]	15
Figure 5 Different types of Robots	16
Figure 6 IRB 6600 axis nomenclature	17
Figure 7 Robot in automation line	17
Figure 8 Nabtesco RV-42N (precision.nabtesco.com 2019)	18
Figure 9 Nabtesco RV Series Gearbox with labels [42]	18
Figure 10 Section view of ACBB [56]	19
Figure 11 Angular Contact Ball Bearing (SKF Media Finder 2019)	19
Figure 12 Cylindrical Roller Bearing	20
Figure 13 section view of CRB (skf.com 2019)	20
Figure 14 section view of TRB (uk.rs-online 2019)	21
Figure 15 Tapered Roller Bearing	21
Figure 16 The Relationship of Velocity and Displacement with constant acceleration	22
Figure 17 Sensors' Mount and Sensitivity Deviation (Modalshop.com 2019)	23
Figure 18 Force and Transfer Path [24]	25
Figure 19 Time and Frequency representation	26
Figure 20 FFT-Analysis of a (a): swept sinusoidal with (b): constant sampling frequency and with (c): speed-synchronously sampling frequency [27]	27

Figure 21 Frequency Spectrum of a single stage gearbox without noise (own representation)	27
Figure 22 Row 1: 20.5 cycles sinusoidal signal with its frequency representation.....	28
Figure 23 Low pass filter (siemens.com 2019)	29
Figure 24 Image 1: Red is raw vibration signal and dotted is the enveloped signal	29
Figure 25 TSA performed on multiple acquired samples (matlab.com 2019)	30
Figure 26 Test Rig.....	33
Figure 27 Signal Acquisition Kit	34
Figure 28 Sensor placement	35
Figure 29 Method for Vibration Noise Isolation.....	36
Figure 30 Arm rotation Cycle.....	37
Figure 31 Motor rotational velocity with constant high-speed areas marked in red	37
Figure 32 @ptitude Observer Hierarchy	39
Figure 33 Mechanism Block Diagram RV series [42]	41
Figure 34 Willis equation for torque and velocity calculation on Nabtesco RV 42N (own representation)	42
Figure 35 Characteristic Frequency spectrum of a gear assembly in good condition [45].....	43
Figure 36 Rotating Element looseness [46]	44
Figure 37 Broken tooth in time waveform and frequency spectrum [44]	45
Figure 38 Accelerometer 1 with Envelope 4 at constant speed of 2100 rpm	49
Figure 39 Accelerometer 1 with Order Tracking and Envelope 4 running with the Robot Cycle	50
Figure 40 Accelerometer 1 with Binning and Envelope 4 running with the Robot Cycle	50
Figure 41 Acc2 and Acc4 using OT in robotic cycle with E4	51
Figure 42 Acc1 with Envspectrum.....	52
Figure 43 Difference between new Gearbox and worn with OT and E4 using the robotic cycle	53
Figure 44 Dismantled Nabtesco RV-42N.....	54
Figure 45 Difference in wear on input pinion, constant speed at 1050 rpm with Order Tracking and Envelope 4.....	55
Figure 46 section view of CRB with outer ring specified (skf.com 2019)	55
Figure 47 Artificial damage to ACBB outer ring	56
Figure 48 Artificial damage to the integrated CRB outer ring	56
Figure 49 Artificial Damage on to Disk undulations	56
Figure 50 Damaged gearbox frequency response at constant speed of 2100 rpm	Error!
Bookmark not defined.	
Figure 51 Damaged Gearbox with Order Tracking of raw data with robotic Cycle	Error!
Bookmark not defined.	
Figure 52 KNIME PCA workflow	59
Figure 53 PCA output plot with model built with Good data	60
Figure 54 Data points from Cluster 1 and Cluster 3 in frequency spectrum (orders) after the Binning Algorithm	61
Figure 55 Data points from Cluster 2 in frequency spectrum (orders) after the Binning algorithm	61
Figure 56 all accelerometers with OT and E4 at constant speed of 1050 rpm without added weight	70
Figure 57 all accelerometers with OT and E4 at constant speed of 2100 rpm with added weight	70

Figure 58 all accelerometers with OT and E2 at constant speed of 1050 rpm.....	71
Figure 59 all accelerometers with OT and E3 at constant speed of 1050 rpm.....	71
Figure 60 all sensors, raw data at constant speed of 2100 rpm.....	72
Figure 61 all sensors with Envspectrum at constant speed of 2100 rpm with amplitude as overall RMS	72
Figure 62 Initial Damage on CRB rollers	73
Figure 63 Initial Damage on the integrated CRB outer ring.....	73
Figure 64 Initial Damage on ACBB outer ring.....	73
Figure 65 Test rig feet with isolation mats	74
Figure 66 Test rig in initial position.....	74
Figure 67 Tachometer placement at input side.....	75
Figure 68 Accelerometer CMS 2200 specifications	76
Figure 69 Tachometer OBR2500-12GM40-E5-V1 technical data	77

List of Abbreviations

• Condition Based Monitoring	CBM
• Condition Monitoring	CM
• Rotating Equipment Performance	REP
• Angular Contact Ball Bearings	ACBB
• Cylindrical Roller Bearing	CRB
• Tapered Roller Bearing	TRB
• Fast Fourier Transform	FFT
• Order Tracking	OT
• Time Synchronous Averaging	TSA
• Spectral Kurtosis	KS
• Envelope1/2/3/4	E1/E2/E3/E4
• Gear Mesh Frequency	GMF
• Disk Mesh Frequency	DMF
• Assembly phase number	Na
• Hunting tooth frequency	HTF
• Assembly phase frequency	APF
• Gear natural frequency	Gnf
• Machine Learning	ML
• Artificial Intelligence	AI
• Principal Component Analysis	PCA
• Deep Learning	DL
• Support Vector Machine	SVM

1. Introduction

As organizations rely more heavily on a small number of technically advanced key machines, equipment condition monitoring has become an increasingly vital way to achieve optimal uptime. However, this wasn't always the case within organizations utilizing large pieces of machinery. According to Maintenance Resources, the history of condition monitoring can be split into three generations spanning from the 1930s to the 1980s and up to current times. [1] During the first generation of evolution, during the '30s and '40s, most factory machinery was relatively basic and there was not as much focus on downtime. In addition, because these tools were less complex, repairs were comparatively simple, carried out much faster than fixes taking place in establishments today.

As machines became more intricate and complicated, companies became increasingly dependent on their industrial equipment. This signaled the beginning of the second generation of equipment monitoring, from the '50s to the '70s. During this time, managers made condition monitoring a higher priority and efforts to reduce downtime became more important. Then, during the third generation that spans from the '80s until today, equipment reliability became a vital focus within any organization that counts on the availability of large machinery. As such, when systems nowadays suffer breakdowns and fail, it can affect the overall functionality and operation of a facility. [1] Thus, a method as predictive maintenance was needed to reduce the effects of sudden failure as shown in figure 1.

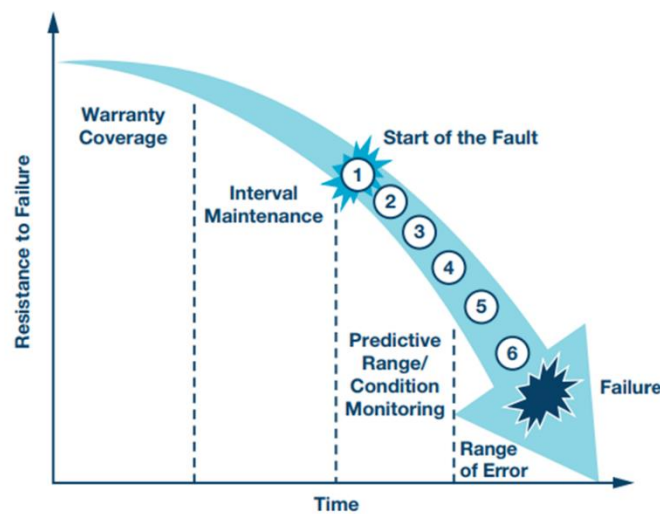


Figure 1 Life Cycle of a machine (analog.com 2019)

Nowadays, in Industry 4.0, it is of utmost importance to get data from running processes and machines which are becoming more complicated. The complexity is increasing especially with the boom of robotics into the manufacturing facilities. This addition brings challenges as in the non-cyclostationary nature and the amount of moving parts in the robot of which the most critical are the gearboxes. High speed variations in the robot's movements and the oscillations, rather than full rotations, in the gearboxes needs consideration. SKF has realized the gap present and has collaborated with Politecnico di Torino in this research topic about condition-based monitoring of a high precision robotic gearbox.

2. Theory

This section provides literature study of the environment of this work starting with the current industry and SKF's involvement in machine monitoring. Robots are introduced and their components from gearboxes and bearings are familiarized. Sensors are then discussed going into the state of the art from previous work and Condition Based Monitoring (CBM). Signal processing and Oil analysis are described coming into Machine Learning (ML) in the field of Vibration analysis. All of which should provide sufficient basis to start with the analysis done in this work.

2.1 Industry 4.0

Manufacturing value chains are complex and technological progress has created several advantages for business world. Industry 4.0 triggers a staggering effect by transforming the manufacturing and production processes in industries. In other words, Industry 4.0 will play a significant role in transforming traditional companies into Smart Factories. A decentralized approach takes great importance in Industry 4.0, which emphasizes independent management of processes and smart objects throughout the network. The development of integrated processes and human machine interaction stimulate complexity and agility but also data transmission between value chains. Through this, industries gain operational efficiency both in time, cost and productivity. Industry 4.0 is the current vision shaping the future of many industries by creating new business models. [2] Figure 2 represents the historical progress from the first industrial revolution leading to industry 4.0.

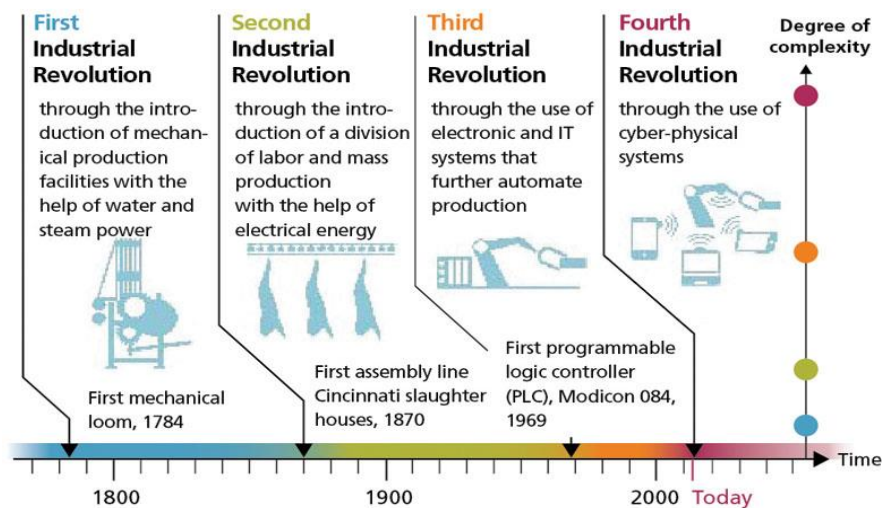


Figure 2 From Industry 1.0 to 4.0 (baimatech.com 2018)

The concept of Industry 4.0 is in the increase of computerized systems, creating more digitized structures and network integration through smart systems. These enable the presence of autonomy in the work environment and conformity of all the production instruments. [2]

2.2 SKF and Rotating Equipment Performance (REP)

SKF has long been a leader in the rotary machinery world, well known for the bearing manufacturing and quality. [3] Another aspect of SKF's work is the continuous monitoring of those rotary components which combines the needs of this new environment, Industry 4.0, and the research work on robotic monitoring.

2.2.1 Vision and Strategy

The concept of CBM for SKF and their high usage of rotary equipment is used in SKF's Rotating Equipment Performance (REP) vision. CBM and Condition Monitoring (CM) has grown in time, initially used on elements rather than products, and has developed into the REP model shown in figure 3 which provides major benefits listed below. [4]

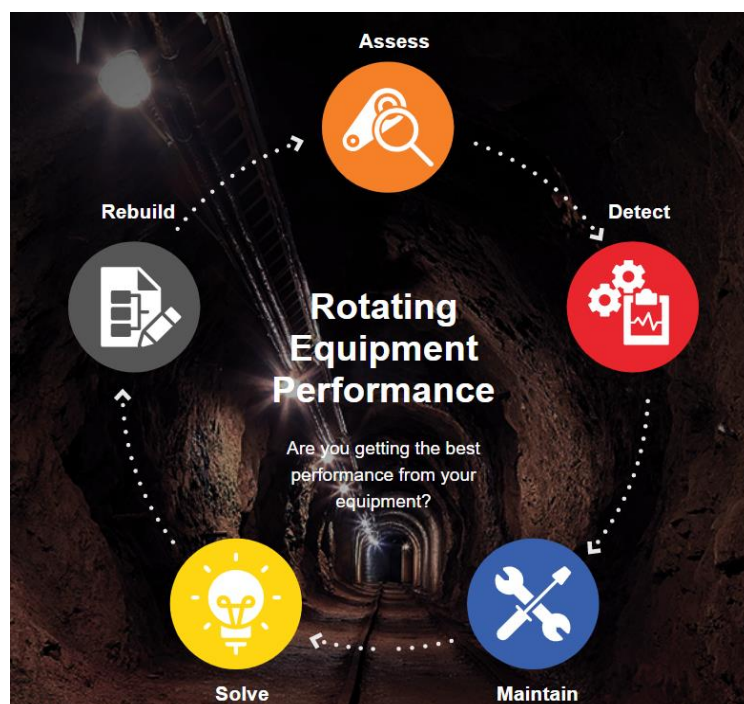


Figure 3 Rotating Equipment Performance
(skf.com/REP 2019)

- Improved Output, done by optimizing the performance of the rotating equipment which can increase availability, performance rate and quality.
- Trim the total cost of Ownership, since poor performance and unplanned downtime don't just affect the productivity and cost of production, they also affect the cost of energy, maintenance, spare parts, labor and more.
- New insights into the machinery through visibility of the health of equipment turning data into performance driving insights.
- Reduce reliance of scarce talent by connecting SKF's rotating equipment expertise, reduction in time and cost of recruiting, training and retaining increasingly scarce and expensive maintenance and diagnostic skillsets.
- More safety in operation due to reduced incident rate and therefore the product safety risks.

- More sustainability where REP can reduce energy usage, waste output and spare parts consumption.

All of which is done through the tasks shown in figure 3 and explained briefly below.

- Assess: identify areas of improvement by assessment and benchmarking.
- Detect: detect impending machine failures and avoid unplanned downtime through the usage of data acquired from sensors.
- Maintain: daily maintenance using the right tools and mechanical maintenance services.
- Solve: application engineering, lubrication management, spare parts management and root cause analysis to fix problems and stop them from re-occurring.
- Rebuild: rebuild services to extend asset life, reduce maintenance costs and improve sustainability.

The steps mentioned above leads to a cycle improving every time used to enhance the REP vision.

2.2.2 Implementation

The goal of these implementations is to transform the maintenance from the preventive to the predictive on the machines utilizing the whole life cycle of the parts, the removal of not needed disassembly and to plan ahead of time the maintenance are some of the benefits. Figure 4 shows an online CM system implemented in Piteå, Sweden. The system measures data simultaneously and emits an alarm at the slightest change in performance, thus increasing the level of control over the condition of the machinery. [5]



Figure 4 Condition Monitoring system in Sweden [5]

2.3 Robotics

After defining the industry and how SKF has a foot in monitoring rotary equipment, the next step is to define robots and their components referring to ISO 8373:2012 [6]. A robot is an actuated mechanism programmable in two or more axes with a degree of autonomy, moving within its environment, to perform intended tasks. Autonomy in this context means the ability to perform intended tasks based on current state and sensing, without human intervention. An industrial robot is defined as an automatically controlled, reprogrammable, multipurpose

manipulator programmable in three or more axes, which can be either fixed in place or mobile for use in industrial automation applications. A robot system is a system comprising of robot(s), end-effector(s) and any machinery, equipment, devices, or sensors supporting the robot performing its task. [6]

2.3.1 Types of robots

Different types of robots exist for different tasks as shown figure 5 where the robots can be separated on basis of function as well as mechanical structure. Although there are several types of robots, the one of interest for this work is the Articulated robot.







					
SCARA	Articulated	Parallel/ Delta	Cartesian/ Linear	Cylinder	Sphere
A SCARA robot is used to install parts or carry items, and is aimed to mimic the activities performed by a human arm. These robots can be used in activities such as automobile factories, underwater construction etc.	These robots use rotary joints to perform activities. They usually have four to six axes, but can have up to 10 axes. Multiple arms are used for these robots in order to ensure greater control or to perform multiple tasks simultaneously.	In a parallel robot, the end-effector is connected to the base through several chains of interconnected links. These robots are of two types – the telescoping-leg hexapod used in most motion simulators and the Delta robot, generally used for rapid pick-and-place activities.	Cartesian robots, also called linear robots, use motors and linear actuators to position a tool. They have three principle axis that move in a straight line rather than rotating.	These robots have three axes of movement – two of which are linear and one circular. Thus, cylinder robots can move along Z and Y axes and rotate along Z axis, and form a cylindrical coordinate system. Hence it has a cylindrical work envelope.	These robots are stationary robot arms having a spherical base and two rotary joints and one linear joint. The spherical base allows these robots to work in a spherical coordinate system. These robots are also known as polar robots.

Figure 5 Different types of Robots
[7]

2.3.2 Articulated Robot

The articulated robot as defined by ISO 8373:2012 [6] by its mechanical structure is a robot whose arm has at least three rotary joints. The articulated robots are mainly used in manufacturing lines, where their flexibility allows them to bend in different directions. Figure 6 shows an articulated robot's axis nomenclature and figure 7 shows the robot in the working environment. In order to function, the components are plenty but what is of interest for this work are the gearboxes that are used within each axis.

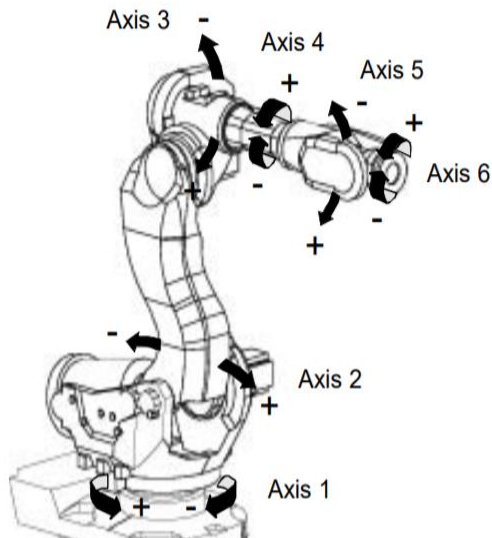


Figure 6 IRB 6600 axis nomenclature [55]

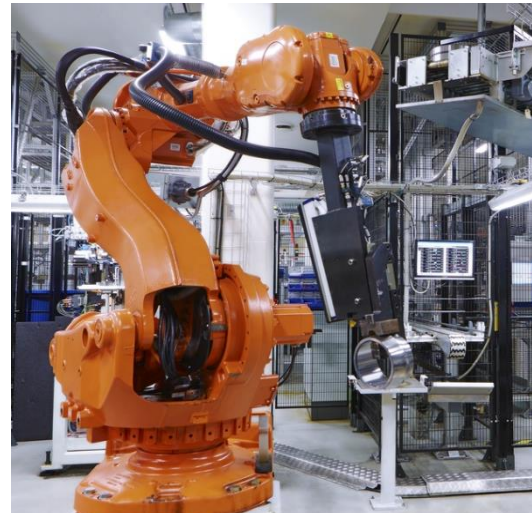


Figure 7 Robot in automation line (SKF media finder 2013)

2.4 Gearboxes

In general, a gearbox is a series of gears contained in a housing also be called a gearhead or gear reducer. It acts as a transmission system mostly to deliver a reduced speed and increased torque to the output. It consists of gears mounted on shafts rotating with the presence of bearings. They are found in any rotary motion that needs power transmission. [8] Gearboxes are used in robots, specifically in the axis of the robots where section 2.4.1 gives a brief introduction of robotic gearboxes going into the Nabtesco RV 42-N.

2.4.1 Robotic Gearboxes

In a robot, gearboxes make up a big part in the cost of the whole robot, around 36% of the total cost. [9] The most used types are cycloid and harmonic drive designs, however planetary gearboxes in addition to spur gear stages and motor only systems in selected axes are now becoming more available with newcomers. [9] The gearboxes used are specifically designed for the tasks to be done as is the Nabtesco RV 42-N.

2.4.2 Nabtesco RV 42-N

Knowing that Nabtesco has 60% of the market share in robotic gearboxes [9], a gearbox that is used in 20Kg payload robots is the Nabtesco RV-42N. It uses cycloidal drives for use in high load and precision being compact and durable promotes it for the use in robotics. [10]



Figure 8 Nabtesco RV-42N
(precision.nabtesco.com 2019)

It consists of 2 stage reduction. The first stage is a spur gear reduction stage from the input pinion that is fixed onto the motor. The 2nd stage is a hypocycloidal stage that transfers the input speed, reduced even more, and the amplified torque onto the output side. The advantage of 2 cycloidal disks is to negate vibration generation which then would translate through the driven shafts. Figure 9 represents a labeled view of this gearbox and section 5.1 reports the components and their kinematic behaviour.

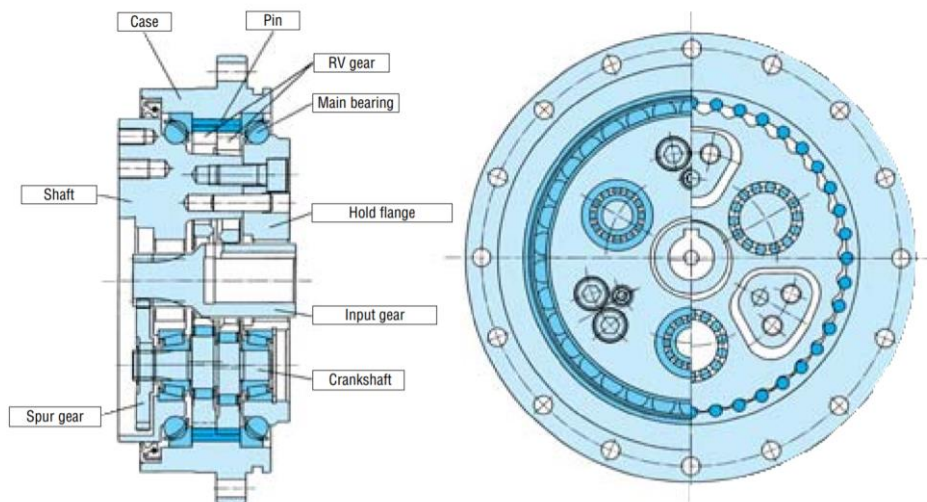


Figure 9 Nabtesco RV Series Gearbox with labels [42]

2.5 Bearings

An important component in this gearbox is the bearings which are machine elements that constrain relative motion to only the desired motion and reduces friction between moving parts. Bearings are classified broadly according to the type of operation, the motions allowed, or to the directions of the loads (forces) applied to the parts. [11] Rotary bearings hold rotating components such as shafts or axles within mechanical systems, and transfer axial and radial loads from the source of the load to the structure supporting it. There are different types of bearings, for each its own benefits of utilization and in this gearbox, are present the Angular Contact Ball Bearings (**ACBB**), Cylindrical Roller Bearing (**CRB**) and Tapered Roller Bearing (**TRB**).

2.5.1 ACBB

Angular contact ball bearings have inner and outer ring raceways that are displaced relative to each other in the direction of the bearing axis. [12] This means that these bearings are designed to accommodate combined loads, i.e. simultaneously acting radial and axial loads. A representation of an ACBB is shown in figure 10 with the contact angle and figure 11 showing the elements.

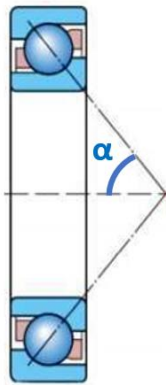


Figure 10 Section view of ACBB [56]



Figure 11 Angular Contact Ball Bearing (SKF Media Finder 2019)

The axial load carrying capacity of angular contact ball bearings increases as the contact angle increases. The contact angle is defined as the angle between the line joining the points of contact of the ball and the raceways in the radial plane, along which the combined load is transmitted from one raceway to another, and a line perpendicular to the bearing axis. [13]

2.5.2 CRB

Rolling bearings support, with minimal friction, rotating or oscillating machine elements and transfer loads between machine components. Rolling bearings provide high precision and low friction and therefore enable high rotational speeds while reducing noise, heat, energy consumption and wear. [14]



Figure 12 Cylindrical Roller Bearing
(SKF Media Finder 2019)

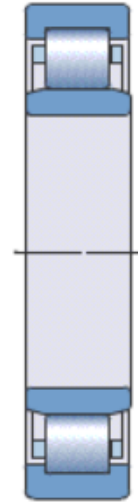


Figure 13 section view of CRB
(skf.com 2019)

Cylindrical Roller Bearings are rolling bearings in which the rolling element is a cylinder rather than a ball as in the ACBB. This provides a larger contact area (linear) rather than a point contact with the outer and inner rings which distributes the loads across a greater surface. They have a high radial load capacity and are favored for high speeds. [15]

2.5.3 TRB

Tapered roller bearings have tapered inner and outer ring raceways as well as tapered rollers. They are designed to accommodate combined loads, i.e. simultaneously acting radial and axial loads. The projection lines of the raceways meet at a common point on the bearing axis to provide a true rolling action and therefore low frictional moments during operation. The axial load carrying capacity of tapered roller bearings increases with increasing contact angle represented in figure 14. [16]

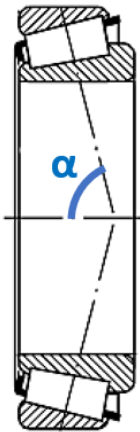


Figure 14 section view of TRB
(uk.rs-online 2019)



Figure 15 Tapered Roller Bearing
(SKF Media Finder 2019)

2.6 Sensors

After stating the components that are going to be monitored, it is important to state the device that is used to acquire the signal emitted starting from the general view of sensors. A sensor is a physical device that measures a physical property or its variation during which it is recorded, responded to or indicated. Sensors may be classified using what physical property they measure as in temperature and humidity sensors. Other classifications may be the operating principle where some are active, require external power, and other are passive, generates output response. For this work, knowing that the task is dealing with vibration monitoring, vibration sensors are those of interest.

2.6.1 Vibration Sensor

For vibration monitoring and analysis, there is a variety of sensors available. The selection of a sensor proportional to displacement, velocity or acceleration depends on the frequencies of interest and the signal levels involved. [17]

Displacement sensors are best suited for measuring low frequency and low amplitude displacements.

Velocity sensors are used for low to medium frequency measurements.

Accelerometers are useful to for measuring low to very high frequencies where the piezoelectric accelerometer is unmatched for frequency and amplitude range.

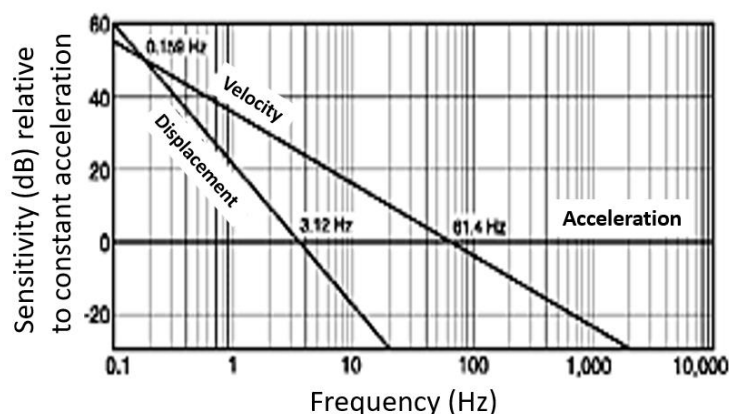


Figure 16 The Relationship of Velocity and Displacement with constant acceleration
(coleparmer.co.uk 2019)

Considering the working condition of monitoring a gearbox and the result shown in figure 16, accelerometers are chosen to be the right choice for the work. However, accelerometers have different ranges depending on their sensitivity in which the operational frequency range varies as shown in the table below.

Sensitivity	Frequency Range
Low (10 mV/g)	10 → 30 K [Hz]
Medium (100 mV/g)	1 → 10 K [Hz]
High (500 mV/g)	0.1 → 2000 [Hz]

Table 1 Accelerometers' Sensitivity and Frequency Range relation [17]

The low sensitivity sensor can detect better at very high frequencies, and the high sensitivity can do so at very low frequencies but due to the application, these ranges are not crucial. The range for the medium sensitivity is the one to be considered. In addition to this, the type of mount of the sensor affects the operational range as shown in figure 17.

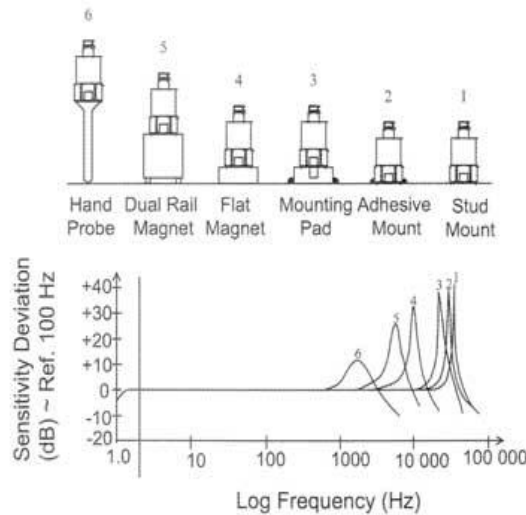


Figure 17 Sensors' Mount and Sensitivity Deviation
(Modalshop.com 2019)

To acquire the maximum range of minimal sensitivity deviation, the stud mount is chosen to be done for all the sensors. Another factor to consider for the accelerometers is the temperature range for operation, but due to having a gearbox, there is already a strict temperature range (maximum 80 °C) which allows the correct operation of the sensors. Thus, the chosen sensors for the vibration measurements are medium sensitivity accelerometers with stud mount.

2.6.2 Temperature Sensor

A temperature sensor is a device that acquires information of the temperature and converts it to an observer. [18] The presence of this sensor is important so that there is no influenced damage to the gearbox's grease which could force a component to be defected in addition to the sensors' temperature limits. The maximum allowable temperature to be seen is 80°C. This is due to the fact that the gearbox can withstand 90°C internally, but the sensor is mounted externally and so 10°C is deducted in order to have a safe operation.

2.6.3 Velocity Sensor

A velocity sensor is a device that measures consecutive position measurements at known intervals and computes the time rate of change in position values. [19] There are many types of sensors that can give the angular velocity of a shaft from AC and DC tachometers to Laser surface velocimeter, all with their own precision, cost and effectiveness. The knowledge of speed and rotations is needed for some signal processing techniques where a velocity sensor is capable in delivering those data.

2.7 State of the Art

In order to move forward with this work, a literature study of the latest research work in the field of vibrational monitoring of gearboxes is needed. Section 2.7.1 reviews the work done in the field of robotic gearboxes, then section 2.7.2 explains the concept of Condition Based Monitoring. After which, section 2.7.3 describes the signal processing techniques then the oil analysis finishing with Machine Learning done in vibration monitoring.

2.7.1 Previous work

The research done in the field of Vibration Monitoring on robotic gearboxes is not broad and so some investigation is needed in order to fill the gap between gearbox monitoring and robotic applications. Previous research work has been already done by SKF in Sweden on an actual robot containing gearboxes of the same operating nature of the one to be tested. [20] [21] However, the results from those work are not conclusive and so a research work on this type of gearboxes is required as an initial step before going on with monitoring on the robot itself.

2.7.2 Condition Based Monitoring

As the industry develops, the term “zero downtime” is becoming more reachable through the implementation and progression of old and novel methods. One of which is Condition Monitoring where nowadays it is charged with developing new technologies to diagnose the machinery problems. Different manners of fault identification have been developed and used effectively to detect the machine faults at an early stage using different machine variables, such as current, voltage, speed, efficiency, temperature and vibrations. One of the principal tools for diagnosing rotating machinery problems has been the vibration analysis. Through the use of different signal processing techniques, it is possible to obtain vital diagnostic information from vibration profile before the equipment catastrophically fails. [22]

Condition Based Monitoring is a type of predictive maintenance that involves using sensors to measure the status of an asset over time while it is in operation. [23] The data collected can be used to establish trends, predict failure, and calculate remaining life of an asset. With CBM, maintenance is only performed when the data shows that performance is decreasing, or a failure is likely.

This method has some limitations as well though as the tools used to monitor equipment for CBM can be expensive to install. Employees must be trained to use CBM technology effectively, which can cost time and money. Furthermore, the sensors employed might not work in harsher operating environments and can have trouble detecting fatigue damage. Although data can be acquired, the analysis and processing of which needs to be done well where section 2.7.3 describes that field.

2.7.3 Signal Analysis and Processing

There are different methods to be used when talking about CBM from the raw time waveform, to the enveloped and order tracked signal. In this section, it is described the vibrational signal acquired in addition to the techniques that are used in this experimental work.

2.7.3.1 Vibration Signal Transfer

An acquired vibration signal does not represent what is occurring inside the gearbox, but rather the vibrations at that specific sensor position. The reason is that the measured vibrational signal is due to the combination of source effects, internal vibrations, and transmission path effects as shown in figure 18. [24]

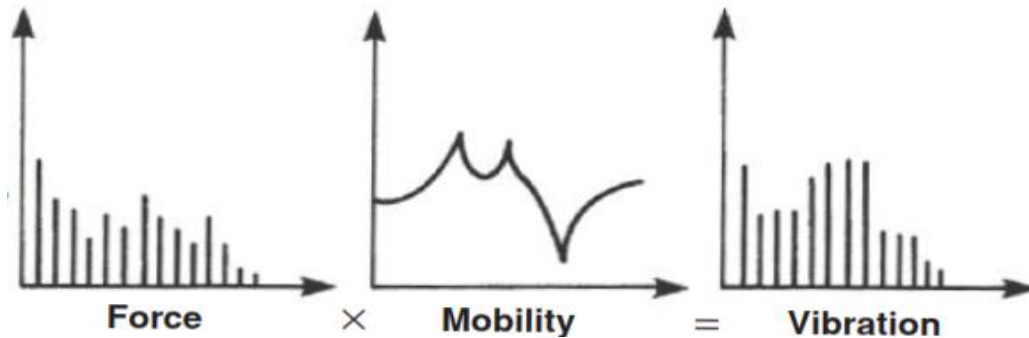


Figure 18 Force and Transfer Path [24]

In addition to that, there is also the presence of the so-called harmonics and sidebands of the original signal source. It can be said that for machines running at constant speed, sinusoidal components in response signals result from sinusoidal forcing functions at the same fundamental frequency. However, due to structural nonlinearities, the responses will usually be distorted from sinusoidal and thus contain some level of harmonics of the fundamental frequency, even if the forcing function is relatively pure. This is the reason why frequency analysis is so powerful as a diagnostic tool, since families of harmonics with a given frequency spacing almost certainly result from a forcing function at that frequency. In a similar way, some effects modulate other frequencies at a lower rate and give rise to families of sidebands around the harmonics of the source frequency. In addition to the transfer path, the presence of structural nonlinearities causes the signal not to be uniquely sinusoidal but rather distorted even if the source is a pure sinusoidal frequency. [24] These factors result in the presence of the so-called harmonics and sidebands of a signal which can be seen in figure 21 in section 2.7.3.4.

2.7.3.2 Time Waveform

This is the method in which it is possible to view the raw signal acquired since it is a plot of amplitude versus time. It shows how the signal changes with time and is very useful to have but does not offer a lot of information about the system's operating frequencies. The time waveform is useful for specific defects that have low frequencies as in a broken tooth where it is possible to visualize such defects as spikes that are significant but don't repeat as frequently. [25] It is also very helpful for pre and post processing of the signal so that it is possible to identify and verify the data acquired.

2.7.3.3 Fast Fourier Transform (FFT)

FFT is a very efficient algorithm to calculate the Discrete Fourier Transform equations. Both the FFT and its discrete counterpart come from the Fourier Series where the basic concept is to express signals as a summation of sinusoidal components where virtually all signals can be decomposed in this way. [24] In machine vibration analysis it is used primarily for periodic signals, as produced by a machine rotating at constant speed. The discretization comes from the need for the signals to be sampled. This corresponds most closely to the Fourier series in that the forward transform is divided by the length of record N to give correctly scaled Fourier series components. However due to the needs of today, the FFT is mostly used due to the reduction in time in the presence of large number of operations. FFT offers a very important tool when analyzing signals especially the repetitive type where rather than visualizing peaks in the time domain, they are viewed as a signal amplitude in the frequency domain as seen in figure 19.

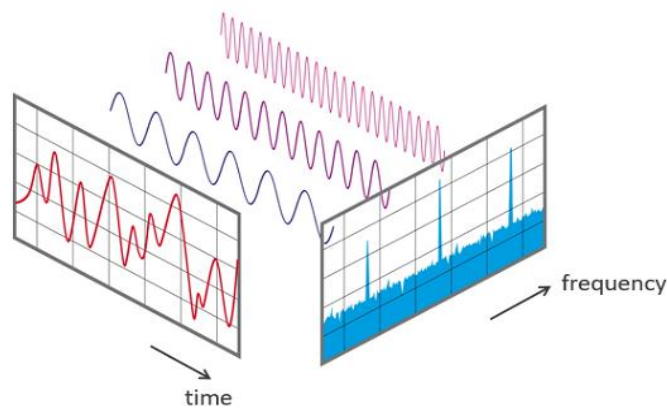


Figure 19 Time and Frequency representation
(nti-audio.com 2019)

2.7.3.4 Order Analysis and Order Tracking (OT)

Orders are harmonics of the rotational speed, and therefore evaluating orders can be critically important on many types of rotating machines especially when the speed is of varying nature. [26] Typically, order tracking and analysis is done on non-stationary data. Basic order analysis, or vibration order analysis, is performed using a fixed sample rate and generating plots of frequency data versus speed. It is common to record the raw time signal and perform post processing on this measurement also.

Order tracking is another method to evaluate orders where it synchronizes the sampling of input signals to the instantaneous angular position of the machine shaft using a resampling technique. Rather than a constant number of samples per time, this results in a constant number of samples per revolution and transforms the analysis to the order domain rather than the frequency domain. Because the orders lie on spectral lines, leakage problems can be avoided. [26]

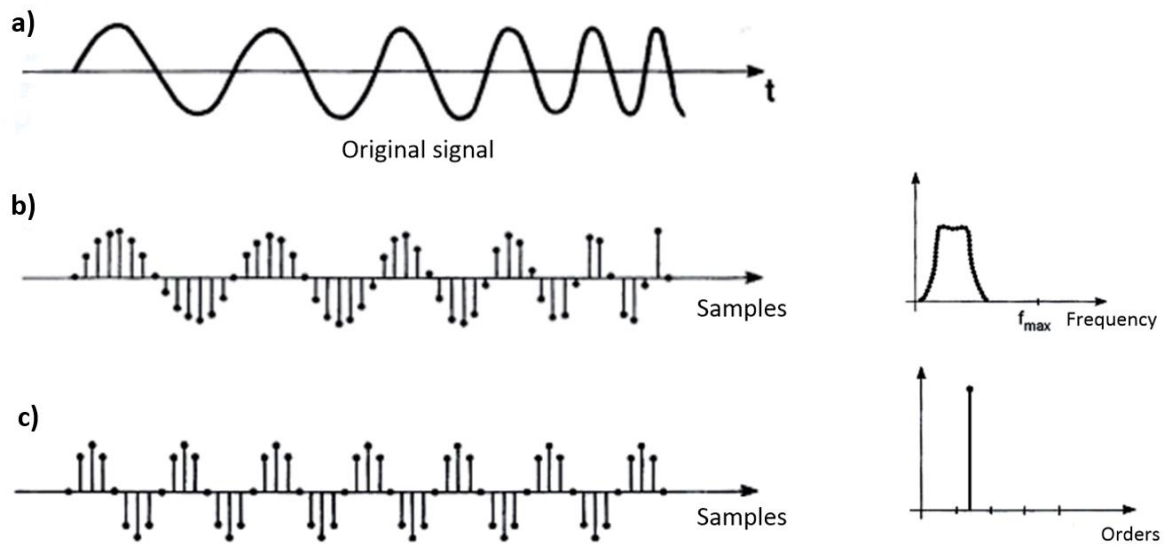


Figure 20 FFT-Analysis of a (a): swept sinusoidal with (b): constant sampling frequency and with (c): speed-synchronously sampling frequency [27]

In addition to the pure signals, there will also be sidebands and harmonics as mentioned in section 2.7.3.1, due to nonlinearities, amplitude modulation and defects. Considering a single stage gearbox with 2 gears, the spectrum will show the input speed, the meshing of the gears as the fundamental frequency with sidebands separated by the input frequency. In addition to that, harmonic signals of the fundamental meshing will be present as seen in figure 21.

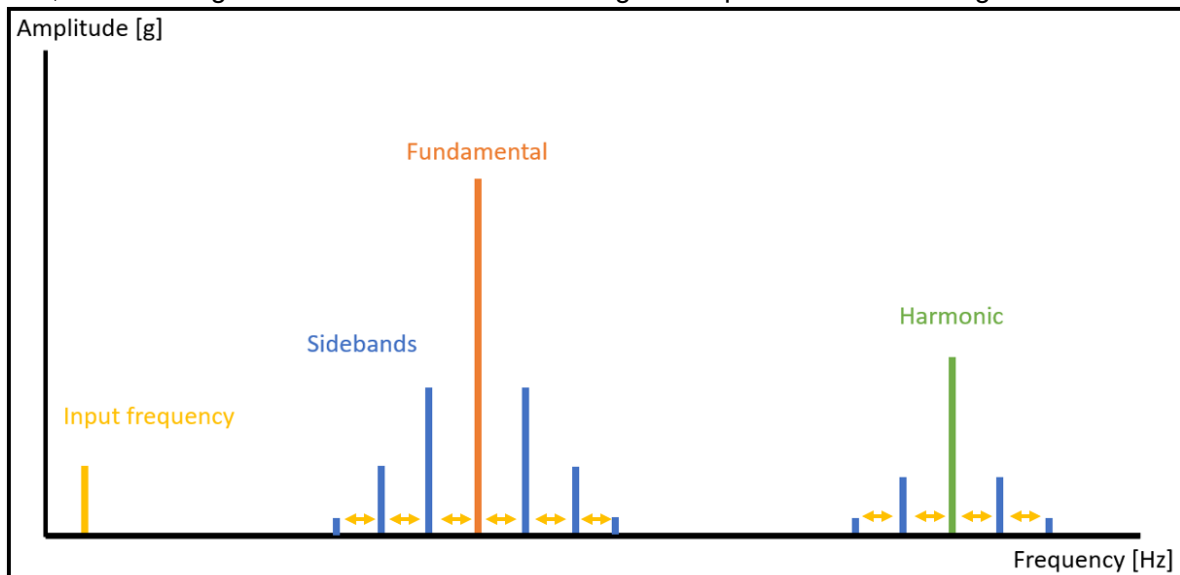


Figure 21 Frequency Spectrum of a single stage gearbox without noise (own representation)

2.7.3.5 Windowing

The utilization of FFT is essential, however a problem rises since it is considered that the sinusoidal signals' cycles are of integer value, but the endpoints are not always continuous. That might cause what is known as spectral leakage where the spectrum you get is not the original one but a smeared one. To minimize the effects of performing an FFT over a non-integer number of cycles it is used a technique called windowing. It reduces the amplitude of

the discontinuities at the boundaries of each finite sequence acquired by the digitizer. [28] It consists of multiplying the time record by a finite-length window with an amplitude that varies smoothly and gradually toward zero at the edges. This makes the endpoints of the waveform meet and, therefore, results in a continuous waveform without sharp transitions. Multiple types of windows are present with the Hanning Window being the most used in these applications where an example is shown in figure 22.

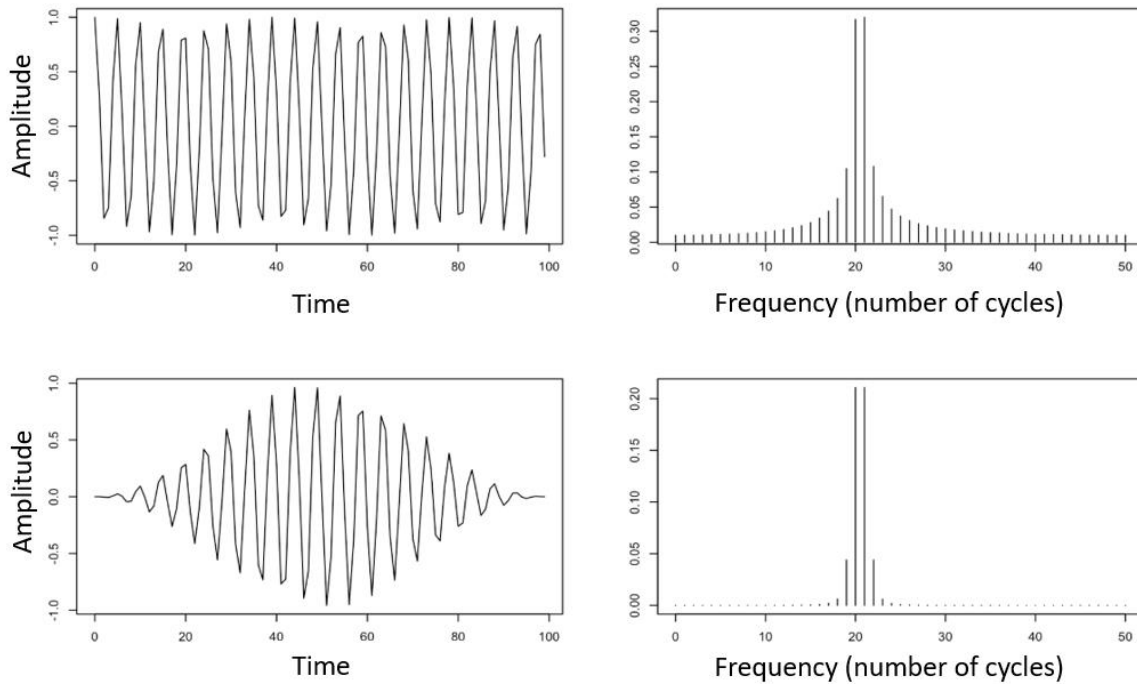


Figure 22 Row 1: 20.5 cycles sinusoidal signal with its frequency representation
Row 2: Same signal with Hanning Window applied [29]

2.7.3.6 Filters

The main purposes for using a filter are to achieve either separation of signals that have been combined or to restore a signal that has been distorted. The main types of filters used are the low pass, high pass, band pass and band reject filters. An important utilization of filters in the field of signal processing is the anti-aliasing filter in addition to enveloping which is discussed in section 2.7.3.7.

Aliasing is when a signal is sampled and then viewed in higher frequency range than half of the sampling rate. Nyquist criteria implements to use a sampling rate at least double that the frequency range of the signals being measured so that the signal is not distorted. [17] The chosen factor for sampling is chosen as 2.56 times the frequency range so that the acquired signals mimic the real. To achieve the Nyquist criteria, a low pass filter is used, an example of which can be seen in figure 23, that filters out the out of range signals.

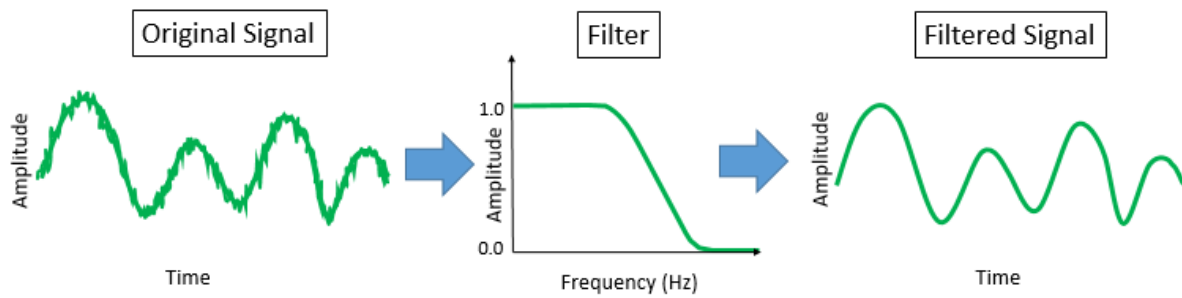


Figure 23 Low pass filter (siemens.com 2019)

2.7.3.7 Enveloping

Enveloping is a method used to remove the signals that are not important to the monitored system and to intensify the frequency range where the signals needed to be detected lie in. Enveloping usually starts with a band pass filter, after which the signal undergoes some rectifying then a low pass anti-aliasing filter. [17] The modulation that occurs on the signal allows to better detect the source rather than the effect as shown in figure 24.



Figure 24 Image 1: Red is raw vibration signal and dotted is the enveloped signal
Image 2: Frequency spectrum of raw signal
Image 3: Frequency spectrum of enveloped signal [30]

2.7.3.8 Time Synchronous Average (TSA)

TSA is used to greatly reduce the effects of unwanted noise in the measurement. The waveform itself is averaged and the sampling of the signal is initiated by a trigger pulse. If the trigger pulse is synchronized with the repetition rate of the signal in question, the averaging process will gradually eliminate the random noise because it is not synchronized with the trigger. However, the signal that is synchronous with the trigger will be emphasized. This is the only type of averaging that does reduce noise. [31]

Another important application of time synchronous averaging is in the waveform analysis of machine vibration, especially in the case of gear drives. In this case, the trigger is derived as

one revolution of the gear. This way, the time samples are synchronized in that they all begin at the same exact point in the angular position of the gear. After performing an enough number of averages, spectrum peaks that are harmonics of RPM will remain when non-synchronous peaks will be averaged out from the spectrum as clarified in figure 25. [31]

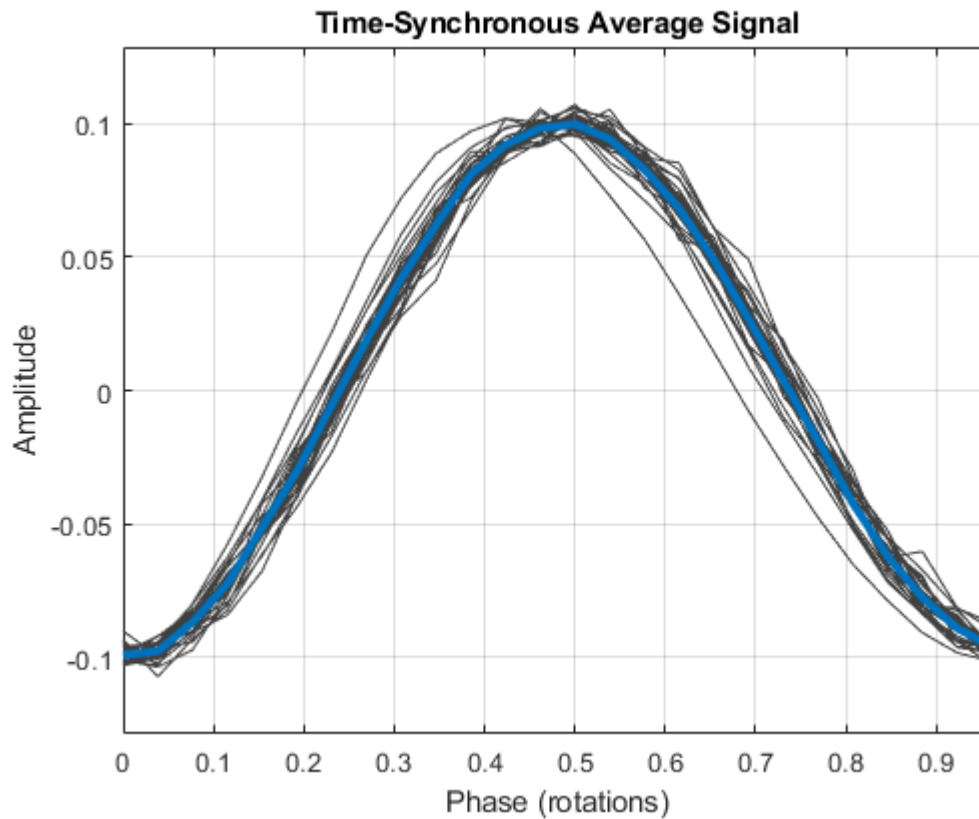


Figure 25 TSA performed on multiple acquired samples (matlab.com 2019)

2.7.3.9 Binning

Binning is an SKF developed algorithm where it is used in the context of condition monitoring for partial rotations. It uses the vibrational signal along with the angular data from an encoder then correlates the two together. It then changes the angular and the vibrational data into angular bins to then have vibrational data with angled bins. Finally, it applies the FFT onto these data and outputs the frequency spectrum. Additional information and full procedure can be found in the confidential work of Verena Slawik [32].

2.7.4 Oil Analysis

Vibration and oil analysis are the two distinct methods in determining mechanical failures in common components of machinery, such as engines, generators and gearboxes. Oil analysis can be categorized into three fluids analysis methods, which are property, fluid contamination and wear debris analysis. Wear debris analysis or analytical Ferrography is a method of predicting the health of equipment in a non-intrusive manner by studying wear particles present in lubricating oil. The subjective determination of component wear is based on the morphological and compositional analysis of wear particles extracted from lubricant oil. It has long been recognized that wear particles are unique and bear individual characteristics, and

they provide significant information for obtaining evidence of the conditions in which they are formed and the wear mechanisms which are prominent. [33]

2.7.5 Machine Learning in Vibration Monitoring

Machine learning is an application of artificial intelligence (AI) that provides systems the ability to automatically learn and improve from experience without being explicitly programmed. [34] Machine learning focuses on the development of computer programs that can access data and use it learn for themselves. The learning algorithm makes it possible to identify patterns in the data, creates models that explain the behavior and to make prediction with the absence of pre-programmed rules and models.

Many publications have been made regarding ML and fault diagnostic especially in bearing faults and the numbers are growing steadily every year. Most of the literature applying the ML algorithms report very satisfactory results with classification accuracy over 90%. Deep Learning (DL) is part of the ML based on neural networks. Deep learning generally requires extremely large datasets. For many applications, including the diagnostics of bearing faults, such large datasets are not readily available and will be expensive and time consuming to acquire. For smaller datasets, classical ML algorithms as Convolutional Neural Network can compete with or even outperform other deep learning networks without the need of add-on architectures. [35]

In addition to those, other research regarding ML and fault diagnosis in gearboxes has been made and has shown positive results which can help being a basis for the work. Artificial neural network, extreme learning machine and Support-Vector Machine (SVM), a new generation learning method based on statistical learning theory, are some of the methods used which are able to classify faults. [36] [37] [38]

In this work, a ML algorithm in the field of anomaly detection will be used called Principal Component Analysis (PCA) with data gathered from a new gearbox and a damaged one. PCA is based on a statistical procedure that uses an orthogonal transformation which converts correlated variables to become uncorrelated variables. [39]

3. Definition

In this section, the target of the work done and the workflow by which to achieve the target will be briefly explained. It is important to clarify these concepts in order to have a clear understanding of why and how some steps are made so that the results can be coherent with the work done.

3.1 Target

The target of this work is to clarify the frequency response of this type of gearboxes since 2 master theses have been done, both unable to show a clear-cut result in the detection of bearing defects or even gear damage. During which, signal processing techniques will be used both on cyclostationary and non-cyclostationary conditions. The results will clarify if possible to apply vibrational analysis and monitoring on this type of gearboxes and if the SKF Binning algorithm provides additional insight. In addition, ML, PCA to be exact, will be used to test the possibility of ML as a first stage of fault detection.

3.2 Workflow

This section provides the logical workflow of this project with more detailed explanation found in chapters 4 and 5. Starting from the test rig setup, the components are studied from the structure of the rig, the sensors used to the signal acquisition kit. The presence of vibrational noise in the premises and how to perform vibrational isolation on the rig. The usage of 2 operational conditions for the gearbox, robotic cycle and constant speed, is possible where the robotic cycle is reported and explained. Chapter 4 concludes with the measurements done and their respective parameters where their application is detailed.

Starting with the analysis, chapter 5, a kinematic study of the gearbox is made starting from the gearbox's parameters. The study provides the different speeds of the components and the torque amplification mechanism. Then comes the identification of the vibrational frequencies that are generated by the gearbox, in terms of good condition and defective conditions. The initial results, their analysis, what they represent, and their interpretation is reported. Some peculiar results are present where they are placed and explained.

After these steps, the gearbox is dismantled, the defects are then chosen and made with the knowledge of what they each represent. The next step is to visualize these frequencies in the frequency spectrum as clear as possible. The difference between all the signal processing techniques used and the 2 operational conditions are reported.

Chapter 5 concludes with ML where an anomaly detection algorithm called PCA is used on a new gearbox and a defected one with different grease. The algorithm is capable of differentiating the two gearboxes forming clusters in its respective plot. The results are reported and interpreted as well as some points who are not within the clusters found. Then a brief conclusion regarding PCA and the result is made before the conclusion of the whole work is reported.

4. Test Rig

In this Chapter, the testing setup environment will be described, where first it is reported the rig with the vibration acquisition tools. Then, the noise present and the method to provide noise isolation from the surrounding machines is explained. It is present 2 manners of operating the motor of the gearbox, one with constant speed and another with a robotic cycle, the cycle is reported in this chapter. At the end, it is defined the different measurements and their parameters used with the acquisition system.

4.1 Test Rig Setup

Starting with the setup, the test rig used is a metallic table bolted to the ground. On the table, the assembly of the electrical motor connected to the gearbox using screws and supports is done. The gearbox has an arm connected to it where at the end of the arm, plates are placed to simulate a weight load. Outside the rig there is the control panel for the assembly, and the tools for signal acquisition are all connected to a computer installed in are the monitoring software.



Figure 26 Test Rig

Object	Nomenclature/Value
Gearbox	Nabtesco RV 42-N
Motor	KEBA KeDrive DMS2
Weight on Arm	30 Kg
Test Rig Mass	Approximately 2 Tons

Table 2 Test Rig Elements

The kit for the signal acquisition contains the *Multilog™ IMX8 board*, a protocol convertor, power supply, terminal blocks, a router, a power switch and a display. The sensors are connected to this kit and this would relay the data to the software in order to store and visualize the vibration and speed measurements acquired.



Figure 27 Signal Acquisition Kit

In addition to the kit and the *SKF Multilog™ On-line System IMx-8*, the interface is connected with *SKF @ptitude™ Observer*. This system allows rapid data storage on multiple machines where the user can have access to the required information when desired. It also comes with wizards to allow an easy setup to maintain and configure the measurements.

@ptitude™ Observer offers the traditional CM displays as Trend, Phase, Time Waveform, FFT and many others. It also offers tools for live data analysis, historical or data captured during transient stages. The ability to have a combination of plots is also possible. These capabilities deliver a powerful and flexible CM solution.

In addition to that, *MATLAB™* which is a fourth-generation programming language and numerical analysis environment is used to perform post-processing techniques. Standard built-in functions are used as '*filter*', '*abs*' and '*fft*' to create filters, have the absolute value of the data and calculate the frequency using the fast fourier transform. An important function that is

used is the 'Env spectrum', it is a function developed for machine diagnosis which performs the Hilbert Transform in addition to enveloping. [40]

The sensors used for data acquisition are 4 accelerometers and 1 tachometer. These sensors are 3 radial sensors and 1 axial sensor. The sensors are placed as in figure 28 with 'ACC0' a sensor used only for emergency shutdown in case of vibration measurements exceeding the assigned limits. As discussed in section 2.6.1, the 4 used accelerometers all have sensitivity of 100mV/g which is the sensitivity range required for the frequency range needed. The mounting is stud mount in order to acquire the broadest frequency range with lowest sensitivity deviation as seen in figure 17. The placement as seen in figure 28 is done to acquire vibrations from the axial direction, Acc3, vertical radial direction, Acc 1, and horizontal radial direction Acc2 and Acc4. This allowed the acquisition of data in all 3 directions necessary with the sensors' specifications reported in the Appendix A.5.

Sensor	Model
Accelerometers	5 x SKF CMS2200
Tachometer	OBR2500-12GM40-E5-V1

Table 3 Accelerometers and Tachometer used

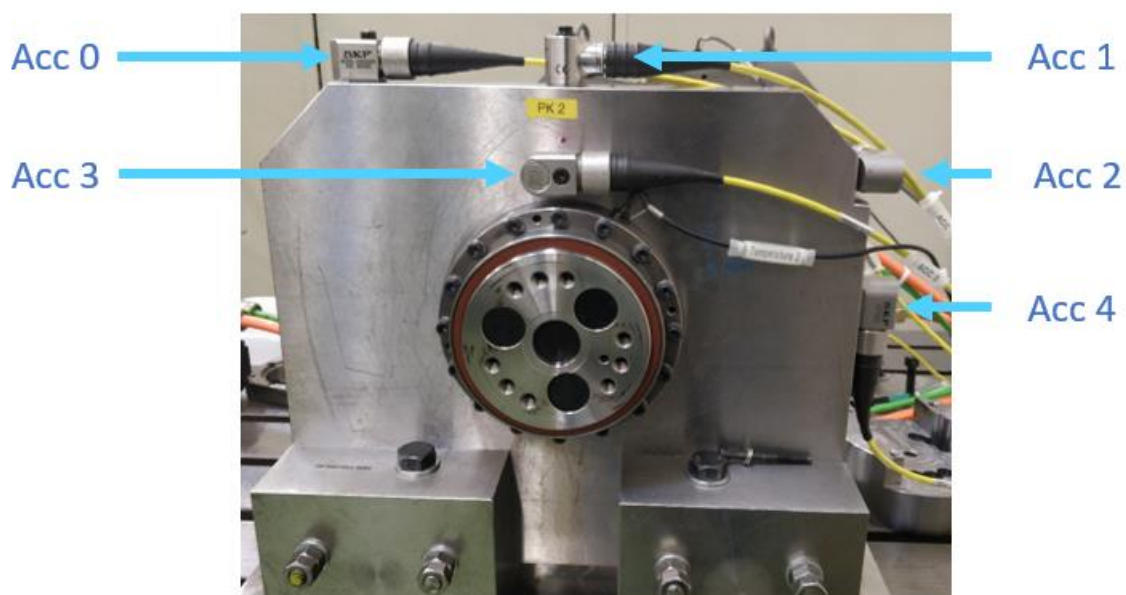


Figure 28 Sensor placement

4.2 Noise Cancellation

Through the first acquisitions, the data acquired shows a lot of noise due to the presence of other machinery in the premises. It is needed to find a solution for this problem and a practical solution is vibration isolation pads as seen in figure 29. The rubber is placed not only between the feet and the ground, but also between the load spreading steel washer and the upper part

of the feet's extensions. This serves as vibration isolation between the test rig and the concrete, which is rugged, low cost and provides large noise reduction.

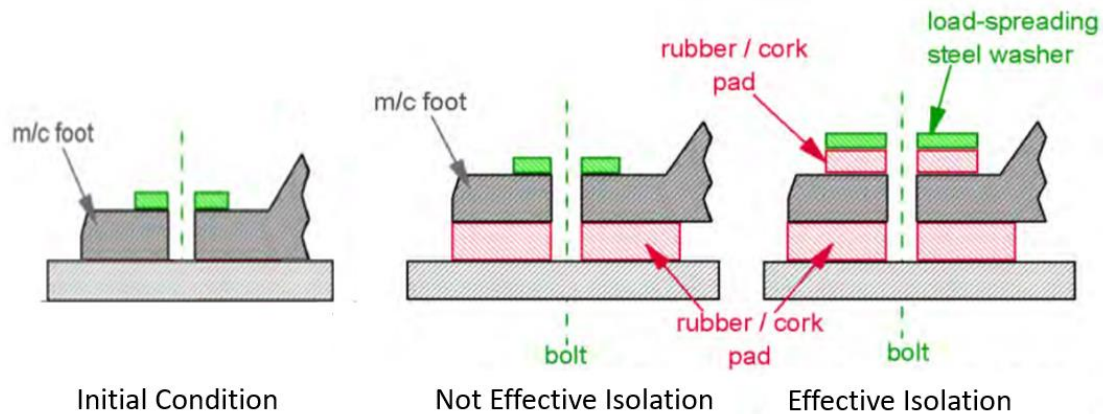


Figure 29 Method for Vibration Noise Isolation
(www.invc.co.uk 2018)

Object	Size
Lower mats	4 16x16x1.3 (cm ³)
Upper mats	4 10x10x1.3 (cm ³)

Table 4 Noise Isolation Mats

To be sure that the mats are qualified for the test rig, the chosen lower mats have to endure both the static and dynamic load. Considering that a mass of 2 tons, the chosen mat is the *Isolierpad Fabcel 200* with 13mm thickness which can endure up to 200 psi. [41] Considering the area of the feet extensions where it will be placed, it would endure up to 18 tons of load which is considered to be acceptable for the test rig. On the upper part of the feet extensions, below the washer, it is needed to have a similar material but with a thinner layer and thus the chosen material is the *Isolierpad Fabcel 50* with 8mm thickness however since the required force for the rods to go through the ground is 50Nm, these mats simply deteriorate and thus the 13mm mats are used. This isolation is deemed crucial and the method used shows good noise cancellation making it possible to continue with the work.

4.3 Robotic Test Cycle

The testing setup allows the possibility of running the gearbox in 2 modes. The first is a non-cyclostationary robotic cycle and the second is cyclostationary at constant speed. The constant speed mode allows the possibility to run the motor at a specific speed that can be altered by the control unit. This mode has no restrictions in terms of revolutions in the input side and is used to verify the data that are acquired from the non-cyclostationary mode.

The robotic test cycle chosen is made to simulated harsh conditions on the gearbox so that it is possible to cause damage upon it. It is taken from *ABB RobotStudio* where an actual robot containing the gearbox is simulated and the cycle represents the axis with the most load during the cycle, axis 2 in figure 6. Thus, this test cycle is chosen to be used which has a rest time of

3 seconds to avoid overheating shown in figure 30 and figure 31 shows the speed variation focusing on the test cycle.

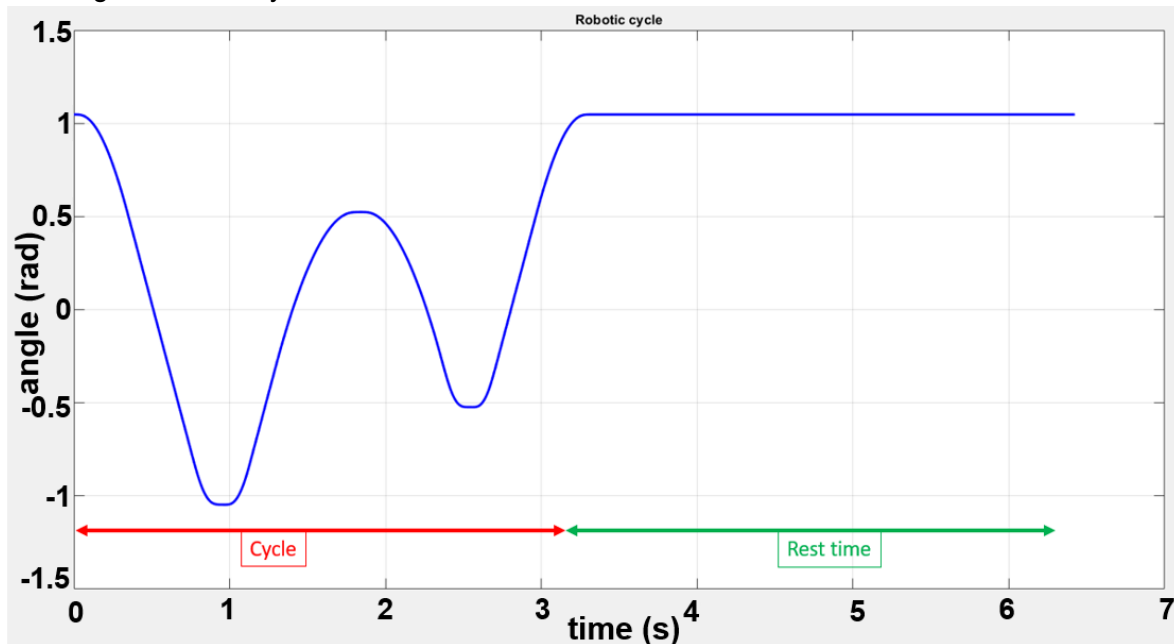


Figure 30 Arm rotation Cycle

In terms of input speed, figure 31 below shows the variations of speed. It shows that for low speed, not a lot of rotations are happening, but there are some constant high speed areas where it would be possible to acquire clear data.

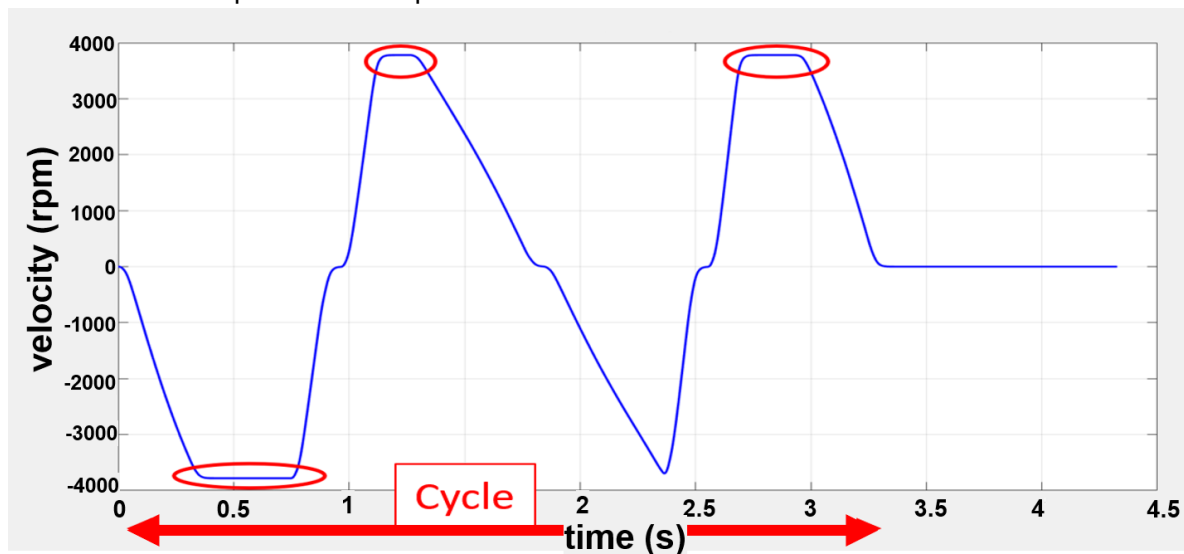


Figure 31 Motor rotational velocity with constant high-speed areas marked in red

4.4 Measurements' Parameters Setup

It is important to specify the measurement points taken for each accelerometer placed regarding the test cycle used. The tools used provide the ability to acquire raw signals, enveloped, order tracked signals and many others but these 3 are of interest. For each sensor, the same measurement points are taken and used. It is selected a wide range of measurement

points but the most useful after testing are reported below. Note that some points for constant speed, especially using OT, cannot be used for the robotic cycle due to the limitations in revolutions made by the motor. Enveloping is implemented as pre-processing at different frequency ranges as shown below.

Enveloping	Low Pass Filter (Hz)	High Pass Filter (Hz)	Window
Envelope 1 (E1)	100	5	Hanning
Envelope 2 (E2)	1000	50	Hanning
Envelope 3 (E3)	10000	500	Hanning
Envelope 4 (E4)	40000	5000	Hanning

Table 5 Measurements' parameters – Constant Speed

In the case of constant speed, the utilization of OT with enveloping shows good results and the points most used are reported below. Although at constant speed it is possible to go on without order tracking, it is noticed the difference between these measurement points and those used for the robotic cycle.

Envelope	Lines	Revolutions	Order (X)	Resolution (X/line)
Yes – E2	6400	64	100	0.015625
Yes – E3	6400	64	100	0.015625
Yes – E4	6400	64	100	0.015625

Table 6 OT Measurements' parameters – Constant Speed

Considering the robotic cycle, both the enveloped and the raw signals are used. Regarding OT, it is needed to be aware that it is not possible to have more than 100% speed difference from the selected initial speed of the measurement point which limits the revolutions possible. Although at low speed there are the highest torques, the low number of rotations present there limits the acquisition to 16 revolutions at the high-speed range.

Envelope	Lines	Revolutions	Order (X)	Resolution (X/line)	Speed Range (cpm)
No	1600	16	100	0.0625	1900-4000
Yes – E2	1600	16	100	0.0625	1900-4000
Yes – E3	1600	16	100	0.0625	1900-4000
Yes – E4	1600	16	100	0.0625	1900-4000

Table 7 Measurements' parameters - Robot Cycle

In addition to the OT points, acquisition of raw time waveform data is also done with the utilization of 6 measurement points as shown below.

Enveloped	Lines	Frequency Range (kHz)	Measurement time (s)	Resolution (X/line)
No	6400	10	0.64	1.5625
No	6400	5	1.28	0.78125
No	6400	2	3.2	0.3125
Yes - E3	6400	10	0.64	1.5625
Yes - E4	6400	10	0.64	1.5625
Yes – E4	6400	5	1.28	0.78125

Table 8 OT Measurements parameters - Robot Cycle

Also, an *Event Capture* for all 4 accelerometers is set up which allows continuous data collection at a specified frequency for more time than the measurement points. However, the accuracy of the data in terms of amplitude is much reduced due to digitization.

The hierarchy in @ptitude Observer is shown in figure 32 where all the 4 accelerometers have the same measurement points as the first.

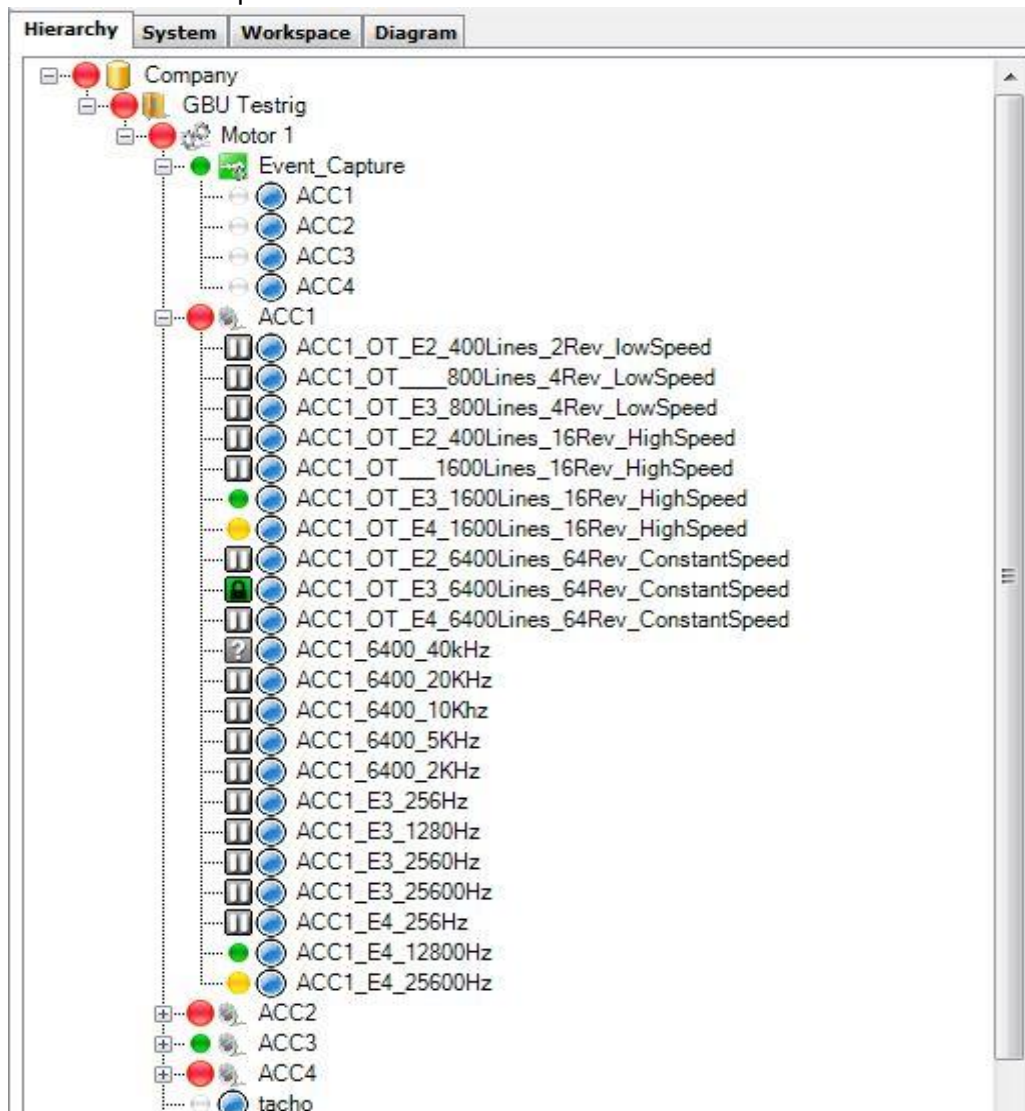


Figure 32 @ptitude Observer Hierarchy

5. Analysis

The knowledge of the testing environment allows to begin the gathering and analysis of the vibration data. The first step is to know the frequencies of the gearbox to later correlate these with the actual extracted frequencies verifying the working state of the gearbox. First, it is stated the kinematics of this gearbox, then the fundamental frequencies for both new and defective gearbox. The results from the data acquisition are presented and interpreted. It is then reported the dismantled gearbox with the artificial defects made and their respective frequencies to be observed. Finally, the ML method and the result are stated and explained which lead to chapter 6 which is the conclusion of the work.

5.1 Gearbox Kinematics

First, it is needed to understand the kinematics of the gearbox and to do so the parameters of this gearbox that are used for this work are listed below. The knowledge of the kinematics of each component is essential so that the frequencies of each part can be known and reported and later, if possible, observed. Table 9 reports the gearbox parameters with a section view found in figure 33.

Parameter	Value/Count
Reduction Ratio	126
Pinion Gears /Input Gear	1
Planet Gears /Spur Gear	3
Cycloidal Disks/RV Gear	2
ACBBs	2
CRBs	6
TRBs	6
Pinion Gear Teeth $Z1$	16
Planet Gear Teeth $Z2$	50
Cycloidal Disk Undulations $Z3$	39
Internal Pins $Z4$	40

Table 9 Nabtesco RV-42N parameters [42]

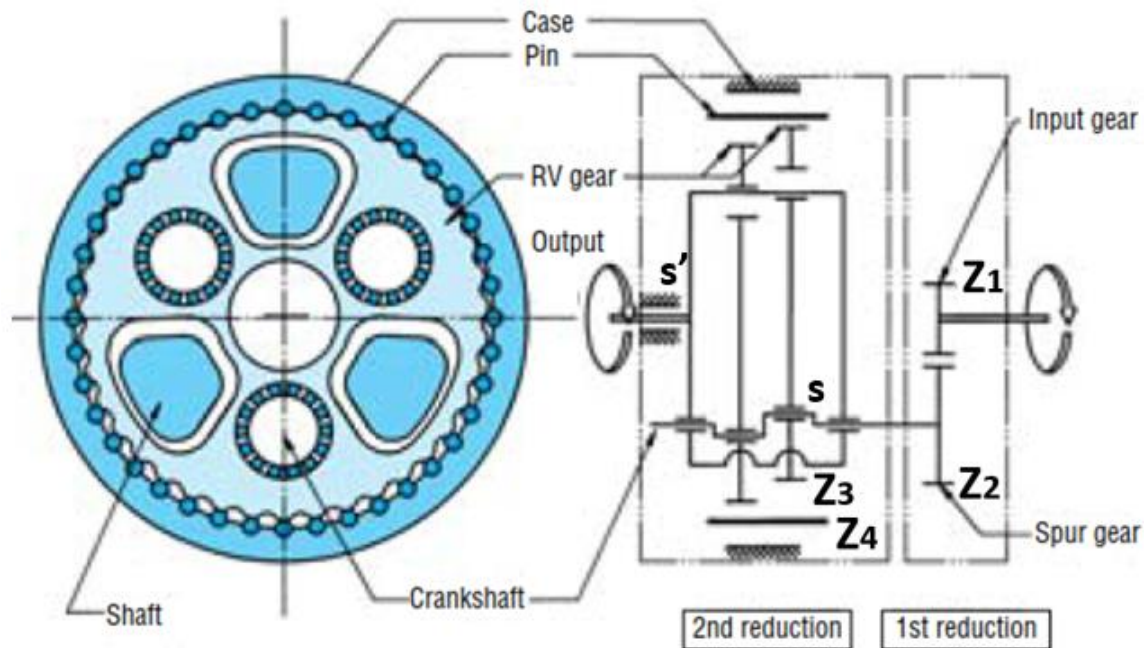


Figure 33 Mechanism Block Diagram RV series [42]

Figure 33 represents the gearbox and its section view with its 2-stage reduction and the gears from the input to the output. The input is through the pinion which rotates the planet teeth which then rotate the Crankshaft which is divided into 2 parts. The first has a TRB connected to the shaft with the inner ring and the outer ring transmits the rotational torque to the overall output carrier. The second part is an excenter which rotates the inner ring of the CRB and transmits the rotation through the outer ring to the Cycloidal disks. The output carrier is connected to the ACBB's inner rings and the outer rings fixed to the gearbox case as is the Hollow/Case with its integrated pins. Regarding the nomenclature seen in figure 33, s refers to the excenter present and s' refers to the output.

Ratio	Value
$i_{1s'}$	126
i_{12}	-3.125
i_{2s}	1
i_{s3}	39
i_{43}	0.975

Table 10 Gear Ratios [42]

In addition to this, a torque and speed study is done using the Willis Equation also known as the fundamental equation of planetary gears. The method shown in figure 34 is done according to the method described by Herbert W.Muller, see [43]

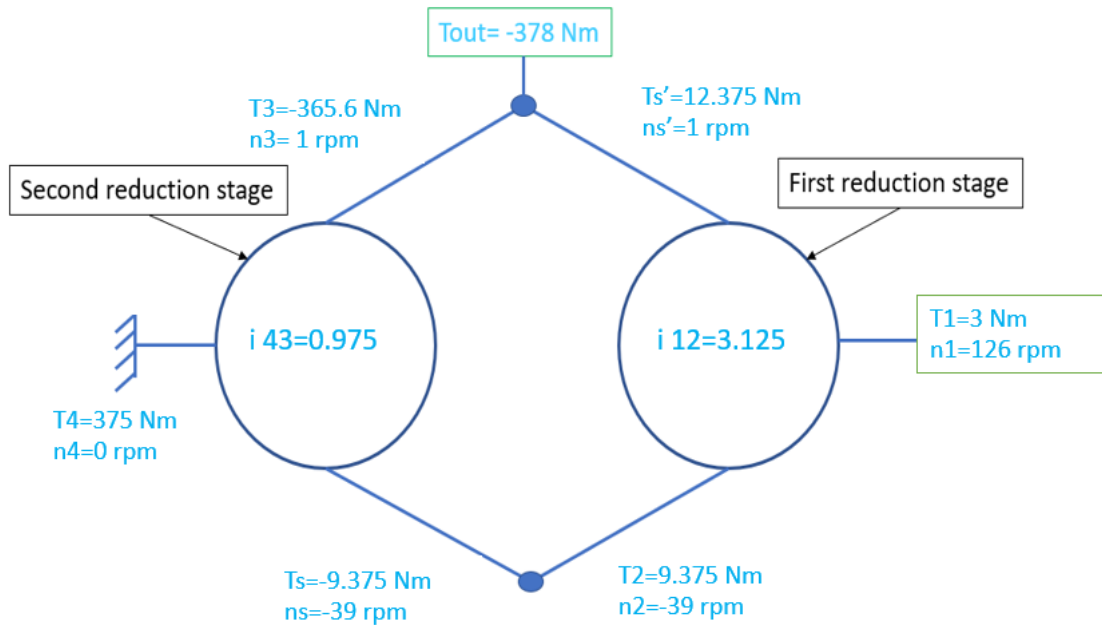


Figure 34 Willis equation for torque and velocity calculation on Nabtesco RV 42N (own representation)

The reduction ratio is then calculated using Z1, Z2 and Z4.

$$i = 1 + \frac{Z2}{Z1} * Z4 = 1 + 125 = 126 \quad (e.1)$$

Knowing that the torque amplification, in the absence of losses, has to be equal to the gear reduction ratio, Willis equation is verified. After the kinematics study of the gearbox, it is required the knowledge of the frequencies of the gearbox, both the fundamental and the bearing defect frequencies.

5.2 Fundamental Frequencies

The rotations inside the gearbox provide vibration signals that are always repeating at a specific rate. Thus, it is possible to calculate these frequencies from the parameters of each vibrating part and then through signal processing techniques, these frequencies can be detected. The frequencies are to be considered relative to the input speed (f_i) also as an x in terms of orders in the frequency equations. Through this method the state of the gearbox and its components can be inferred.

5.2.1 Gears' Frequencies

The operation of the gearbox is due to the input pinion rotating, this is the input speed for all the gearbox and the basis for all the upcoming frequency calculations.

$$f_i = x \quad (e.2)$$

Considering the presence of gears at the input stage and the cycloidal stage, there are two important meshing frequencies which are the **Gear Mesh Frequency (GMF)** and the **Disk Mesh Frequency (DMF)**.

The *GMF* is the frequency of the spur gears meshing at the input stage and is calculated considering the presence of 16 teeth at the pinion gear.

$$GMF = Z1 * fi = 16 * x \quad (e.3)$$

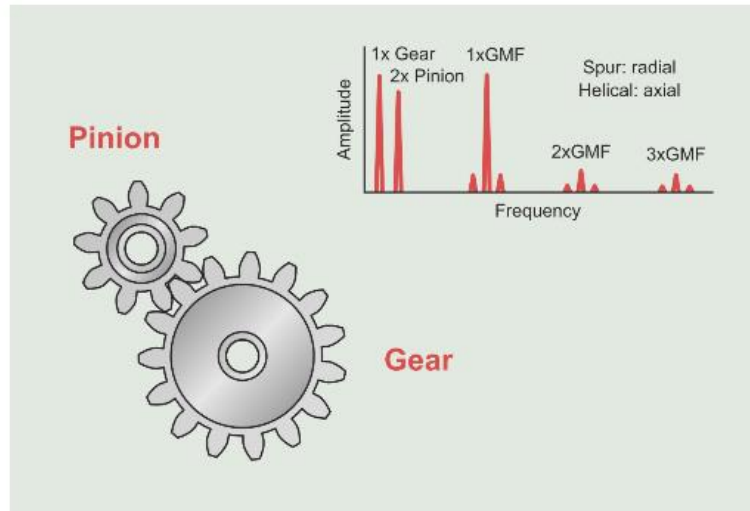


Figure 35 Characteristic Frequency spectrum of a gear assembly in good condition [45]

The *DMF* is the hypocycloid disk mesh frequency which rotates with the same speed as the output and since it has 39 undulations, its frequency is calculated as $Z3$ divided by the reduction ratio of the gearbox.

$$DMF = \frac{Z3}{126} * fi = 0.309 * x \quad (e.4)$$

These frequencies represent the frequencies that should be visible in a perfectly working gearbox having the *GMF* with sidebands of the *DMF* and the input frequency, harmonics as well should be present. [44] Due to the presence of 3 planet gears, the harmonics should have the *GMF*, *2xGMF* and *3xGMF* as the most dominant.

The presence of defects on the gears can also be detected by the frequency range where the **Hunting Tooth Frequency (HTF)** and the **Assembly Phase Frequency (APF)** are present. Na is called the number of assembly phase and is calculated by finding the least common prime between the planet's and pinion's teeth number.

$$Na = 2 \quad (e.5)$$

The *HTF* occurs when there is damage on a tooth of a pinion and the planet where the maximum vibration occurs when both defects contact each other. [45] It is difficult to identify in the frequency spectrum due to having a low frequency value and better seen in the time waveform.

$$HTF = \frac{GMF * Na}{Z1 * Z2} = 0.04 * x \quad (e.6)$$

The *APF* is due to wear where the space between the teeth and the teeth profile has changed. [45]

$$APF = \frac{GMF}{Na} = 8 * x \quad (e.7)$$

In addition to the *APF*, a sign of wear is the increase in amplitude of the sidebands. [45]

Misalignment can be seen in the frequency spectrum as well, its presence can be seen radially as 2x if its axial misalignment and if it is an angular misalignment, it is 1x measured radially. [17]

Looseness rises from multiple of causes, poor mounting, missing components, excessive clearances or an increase of tolerances due to wear. [46] It is seen as high amplitude of the *GMF* and its low harmonics. In the presence of mechanical looseness, there will also be half harmonics present as well.

A special type of looseness is the Rotating Element looseness. This is seen in the spectrum as harmonics, subharmonics (0.5 x) and half harmonics (1.5 x, 2.5 x, 3.5 x). [46] This could be due to excessive clearance within the bearings which leads to if not caused by misalignment.

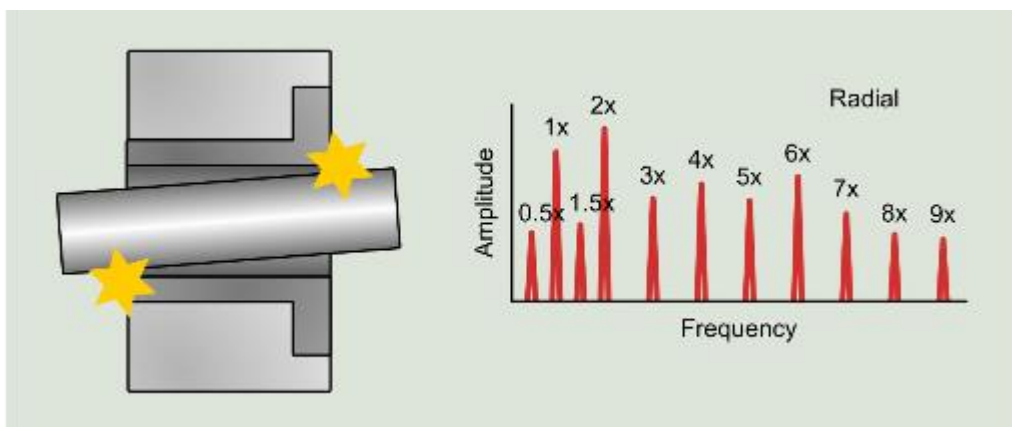


Figure 36 Rotating Element looseness [46]

Wear is one of the most common reasons for gear damage. This includes pitting, corrosive and abrasive wear. It is detected with an increase in sidebands, number and amplitude, and incremental increase in the low harmonics of the *GMF*. [47]

Imbalance is of two types, either static or dynamic. Static is when there is additional mass on one side of the shaft with respect to the center of mass and dynamic is when the imbalance is symmetric with respect to the center of mass. It is seen once with every rotation and in the frequency spectrum it is 1x the input frequency seen radially. [17]

Broken tooth, in the case of the broken tooth, it can be seen as one peak whenever this tooth comes in contact with another, however due to its low frequency, it can be seen better in the time waveform as a spike at every mesh instance of the tooth. In the frequency spectrum, the **Gnf**, gear natural frequency which represents the resonance of the gear, will be present as well. [25]

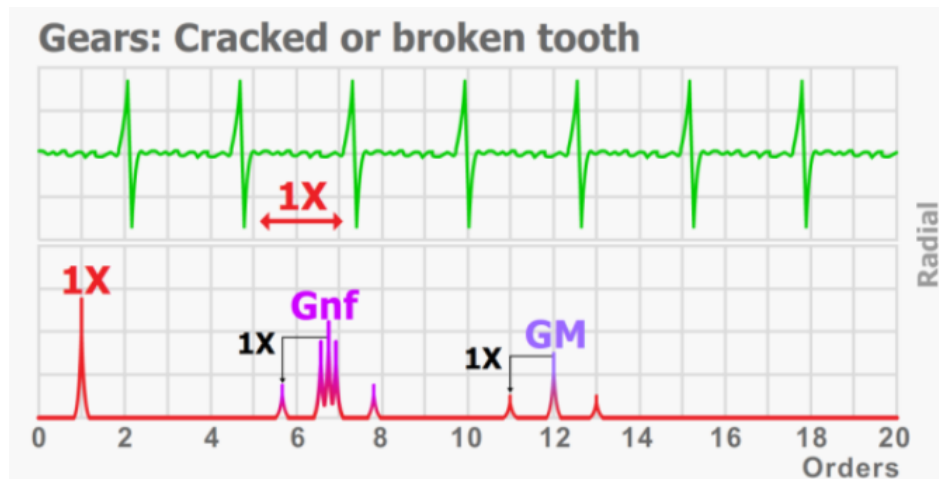


Figure 37 Broken tooth in time waveform and frequency spectrum [44]

After indicating and explaining the fundamental frequencies of the gears and their respective damage frequencies, table 11 summarizes them in a single table.

Frequency source	Repetition Frequency[x]
f_i	x
GMF	$16 * x$
DMF	$0.309 * x$
HTF	$0.04 * x$
APF	$8 * x$
Axial Misalignment	High amplitude of $2 * x$ (seen radially)
Radial Misalignment	High amplitude of $1 * x$ (seen axially)
Looseness	High amplitude of GMF and half harmonics
Wear	Higher amplitude of GMF and sidebands
Imbalance	High amplitude of $1 * x$ (seen radially)
Broken tooth	Presence of Gnf, better seen in time waveform

Table 11 Fundamental Frequencies of Gears

5.2.2 Bearing Defect Frequencies

With respect to bearings, every time a local defect is over-rolled, a pulse-like excitation force is generated. The time between these pulses depends on the rotation speed of the bearing components and the number of rolling elements in addition to the transfer path between the defect and the measured signal will be influenced. [48] The bearings' defect frequencies also have some specific attributes in terms of sidebands that makes it easier to diagnose the fault and its specific type.

Variable
Number of rolling elements (z)
Diameter of rolling element (dre)
Pitch Diameter (dp)
Contact angle (α)
Inner ring rotation speed (fin)
Outer ring rotation speed (fout)

Table 12 Bearings' variables for defect frequency calculations

These variables allow to calculate the rotation frequencies of the components and then of the repetition frequency of the defect location.

Component	Rotation Frequency [Hz]
Cage	$f_c = \frac{f_{in}}{2} \left[1 - \frac{d_{re}}{d_p} * \cos(\alpha) \right] + \frac{f_{out}}{2} \left[1 + \frac{d_{re}}{d_p} * \cos(\alpha) \right]$ (e. 8)
Rolling Element	$f_{re} = \frac{d_p}{d_{re}} (f_{out} - f_c) \left[1 + \frac{d_{re}}{d_p} * \cos(\alpha) \right]$ (e. 9)

Table 13 Rotation Frequencies of cage and rolling element [48]

Then the repetition frequency of the specific defect location is calculated.

Defect Location	Repetition Frequency [Hz]
Inner Ring	$f_{ird} = z f_c - f_{in} \pm f_{in}$ (e.10)
Outer Ring	$f_{ord} = z f_c - f_{out} \pm f_{out}$ (e.11)
Rolling Element	$f_{red} = 2f_{re} \pm f_c$ (e.12)

Table 14 Repetition Frequency of Defect Location [48]

The presence of \pm is to signify the sidebands of each repetition frequency. [48]

5.2.2.1 ACBB Defect Frequencies

The knowledge of the ACBB being on the output side provides the information that its defect frequencies will have much lower frequencies with respect to the other bearings that are connected to the input side of this high reduction gearbox.

Variable	Value
Number of rolling elements (z)	36
Diameter of rolling element (dre)	7.938 mm
Pitch Diameter (dp)	111.016 mm
Contact angle (α)	40°
Inner ring rotation speed (fin)	0.008 * x (e. 13)
Outer ring rotation speed (fout)	0

Table 15 ACBB variables for defect frequency calculation

This allows the calculation of the defect frequencies.

Component	Rotation Frequency (orders)
Cage	$0.00375 * x$ (e. 14)
Rolling Element	$0.055 * x$ (e. 15)
Defect Location	Repetition Frequency (orders)
Inner Ring	$0.15 * x$ (e. 16)
Outer Ring	$0.135 * x$ (e. 17)
Rolling Element	$0.11 * x$ (e. 18)

Table 16 Rotation and Repetition frequencies for ACBB components

These frequencies show that if a defect is to be present on the ACBB, it is difficult to identify due to their low frequency range.

5.2.2.2 CRB Defect Frequencies

The CRB is the component closest to the Cycloidal disks which are connected to the inner ring of the CRB and the outer ring is connected the same shaft as the excentre. The same procedure as done for the ACBB will be made here in order to acquire the defect frequencies.

Variable	Value
Number of rolling elements (z)	14
Diameter of rolling element (dre)	3.735 mm
Pitch Diameter (dp)	24.23 mm
Contact angle (α)	0°
Inner ring rotation speed (fin)	$-0.31 * x$ (e. 19)
Outer ring rotation speed (fout)	$0.008 * x$ (e. 20)

Table 17 CRB variables for defect frequency calculation

In the table below, it is reported the defect frequencies of bearing components and location.

Component	Rotation Frequency (orders)
Cage	$-0.13 * x$ (e. 21)
Rolling Element	$1.005 * x$ (e. 22)
Defect Location	Repetition Frequency (orders)
Inner Ring	$2.56 * x$ (e. 23)
Outer Ring	$1.88 * x$ (e. 24)
Rolling Element	$2.01 * x$ (e. 25)

Table 18 Rotation and Repetition frequencies for CRB components

5.2.2.3 TRB Defect Frequencies

Similar to the ACBB and the CRB, the TRB's dimensions are measured to acquire the defect frequencies.

Variable	Value
Number of rolling elements (z)	13
Diameter of rolling element (dre)	3.4 mm
Pitch Diameter (dp)	19.39 mm
Contact angle (α)	8.8°
Inner ring rotation speed (fin)	$-0.31 * x$ (e. 26)
Outer ring rotation speed (fout)	$0.008 * x$ (e. 27)

Table 19 TRB variables for defect frequency calculation

Then the defect frequencies are calculated.

Component	Rotation Frequency (orders)
Cage	$-0.17 * x$ (e. 28)
Rolling Element	$0.91 * x$ (e. 29)
Defect Location	Repetition Frequency (orders)
Inner Ring	$2.36 * x$ (e. 30)
Outer Ring	$1.76 * x$ (e. 31)
Rolling Element	$1.82 * x$ (e. 32)

Table 20 Rotation and Repetition frequencies for TRB components

5.3 Results

First, it is needed to verify the above-mentioned frequencies since the gearbox should show the *GMF*, *DMF* and x . Since it is possible to run at constant speed, it made the results of the robotic cycle easier to verify since there is no variability in the frequency range. The possibility to measure both a new gearbox and a gearbox that had ran 600 hours with the robotic cycle is possible. Initially, they both shared the same results in frequency peaks with different amplitudes which will be reported in the following sections. In addition to that, section 5.3.2 reports the differences in methods used and the effect of weight onto the whole setup.

5.3.1 Initial Results

This section will report the clearest data acquired with the filtering techniques applied in case of constant speed and the robotic cycle. An interpretation of the results will also be made in section 5.3.1.3 of the results acquired.

5.3.1.1 Constant Speed

At this condition, many methods are present and could verify the status of the working gearbox. After many trials, the clearest method directly accessible from the @ptitude Observer is with E4 where the frequency spectrum can be directly observed on the software.

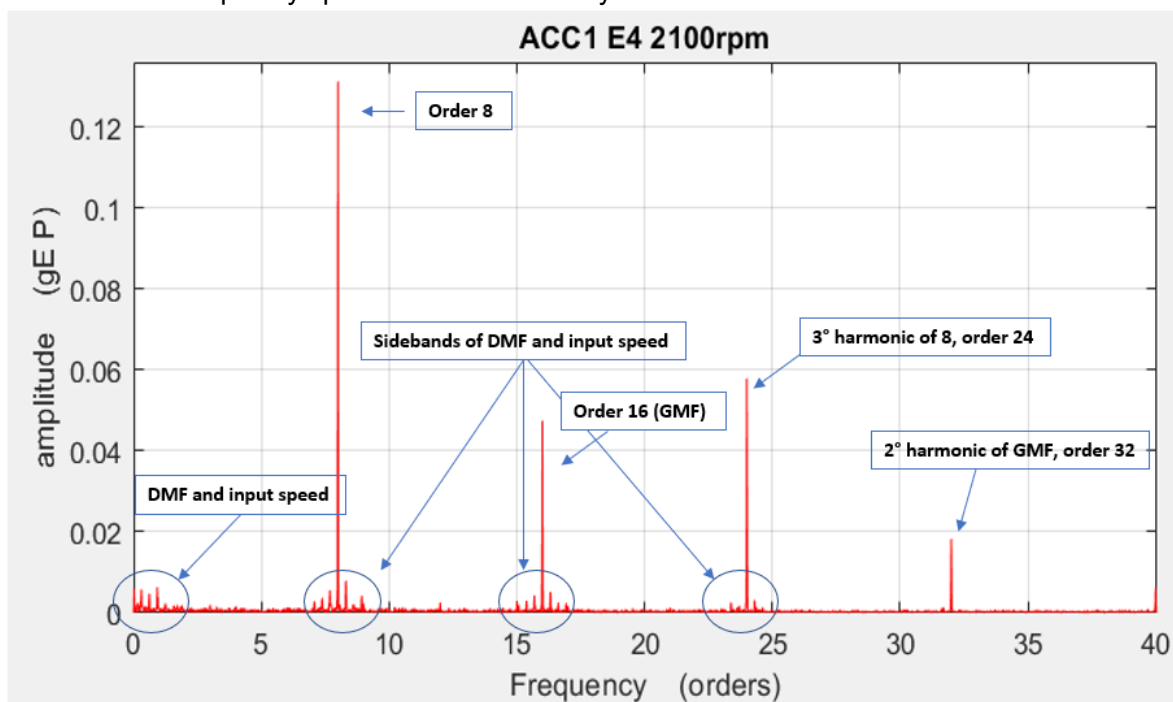


Figure 38 Accelerometer 1 with Envelope 4 at constant speed of 2100 rpm

5.3.1.2 Robotic cycle

Using the robotic cycle, it should now be possible to mimic the data acquired at constant speed with lower accuracy in terms of frequency. The first method is OT with E4, but due to the limitations of this method, the resolution will be much lower due to the limited number of revolutions of the input. This leads to being capable of acquiring reliable data only on the high-speed zones which are not the high torque areas.

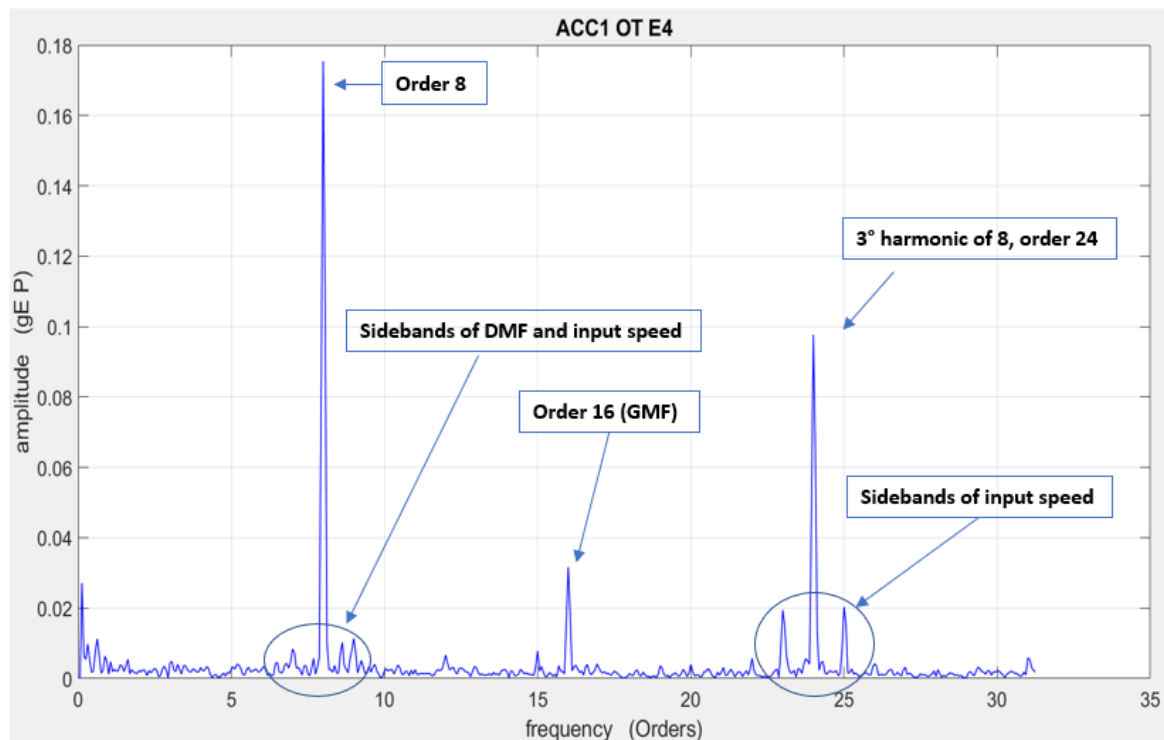


Figure 39 Accelerometer 1 with Order Tracking and Envelope 4 running with the Robot Cycle

The other method that is used is the SKF developed Binning Algorithm and is done as post processing.

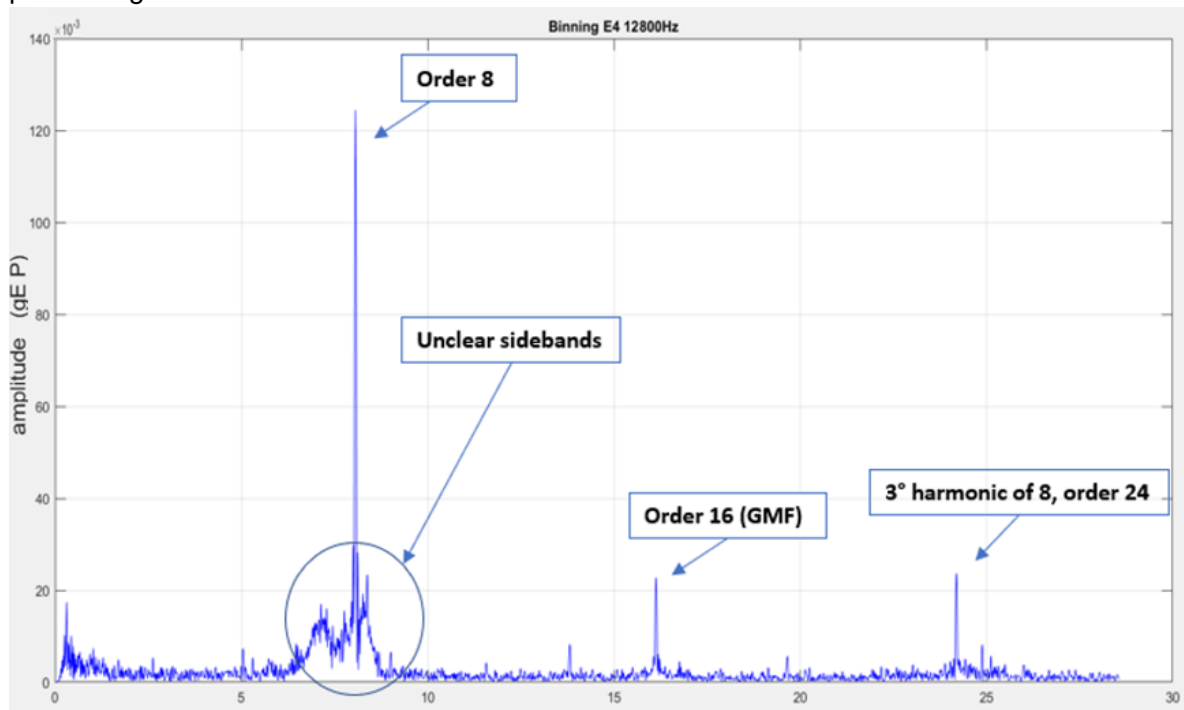


Figure 40 Accelerometer 1 with Binning and Envelope 4 running with the Robot Cycle

5.3.1.3 Interpretation

The acquired data shows peaks at orders 8, 16 and 24. In addition to those, the data shows peaks at the GMF with sidebands representing the DMF and the input frequency at those peaks. The expected frequency range is peaks at orders 16, 32 and 48. 16 being the GMF, 32 and 48 due the presence of three gears. The frequency spectrum represented as 8, 16 and 32 shows that the meshing and torque transfer is occurring as if the input pinion has 8 teeth rather than 16, half of what is expected. This could be due mechanical looseness from within the gearbox or excitation from the motor side with its 8 poles. The presence of 8 poles and 16 teeth as the input gear could have caused vibrations which are seen in the results above. This is further enforced when another gearbox with teeth set number not a multiple of 8 is tested. It shows the presence of orders 8 and 16 in the E3 and E4 but not in the raw data or E2. This reveals that the excitations, being multiple of 8, promote vibrations in the measured data.

5.3.2 Results to mention

In this section, the measurements taken from other sensors, with and without load will be reported in addition to the different acquisition methods and post processing done.

5.3.2.1 Added Weight effect

The reason behind the usage of Acc1 in section 5.2.3.1 is due to instability of Acc2 and Acc4 in data acquisition when the arm with weight is connected in both constant speed and the robotic cycle. The reason behind this is the test setup, it is not fixed in the horizontal direction but rather only in the vertical and axial. This results in many peaks in the frequency spectrum separated with the input frequency as seen in figure 41. All the sensors' results are reported in appendix A.1 using E4 with and without weight.

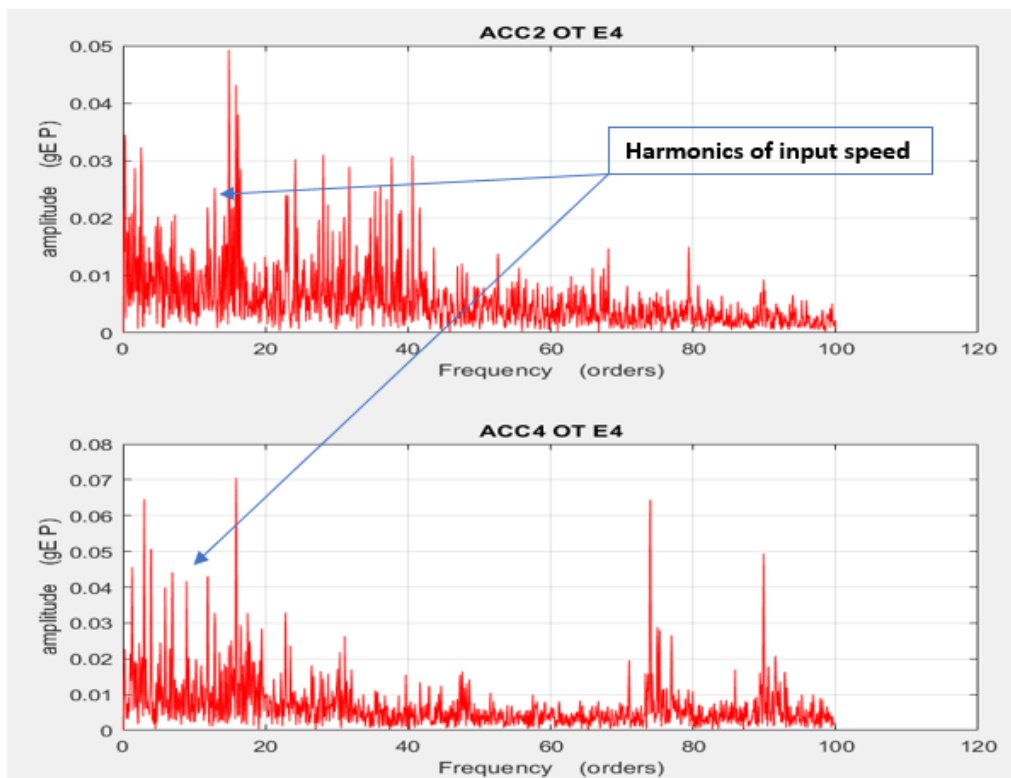


Figure 41 Acc2 and Acc4 using OT in robotic cycle with E4

5.3.2.2 Envspectrum

Initially, the post processing method integrated into Matlab called Envspectrum explained in section 4.3.1 is used and the results are shown below. Although it is considered as a powerful diagnostic tool, the results from the E4 in figure 39 are much clearer in detecting sidebands and more harmonics. In addition, the algorithm built within this function is limited to cyclostationary conditions.

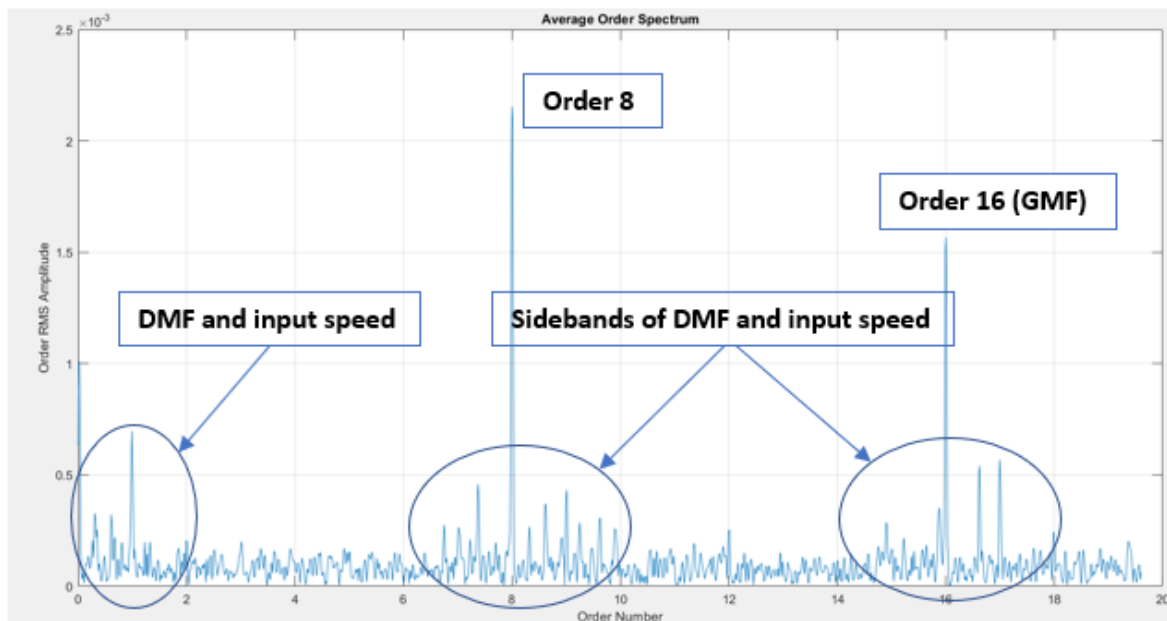


Figure 42 Acc1 with Envspectrum

Considering the presence of other enveloping techniques, the results needed to be reported. The results are all shown in the appendix in section A.2. It is possible to interpret through the reported figures that the envelope chosen, E4, shows the clearest peaks.

5.3.2.3 Difference between New Gearbox and Worn Gearbox

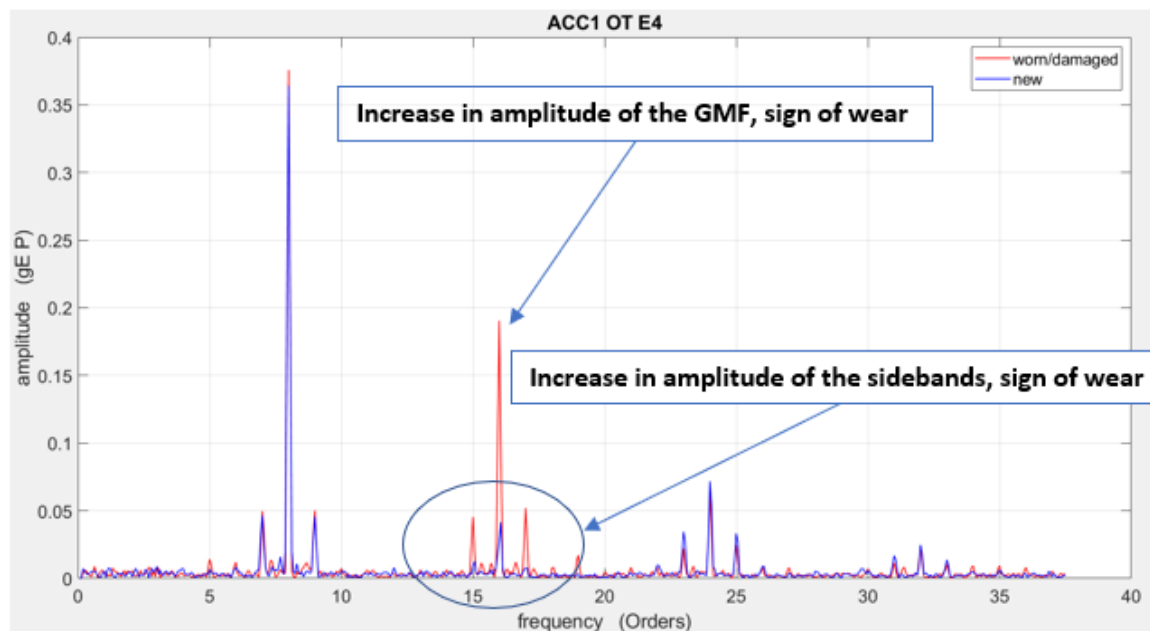


Figure 43 Difference between new Gearbox and worn with OT and E4 using the robotic cycle

The above figure reports the difference between a worn and a new gearbox with the same conditions used. It shows an increase in the amplitude of the GMF and its sidebands. Considering the other frequency orders, no other differences are seen in terms of high differences. This result could clarify that the presence and high amplitude peaks of the 8th with its harmonics comes from outside the gearbox. As discussed in section 5.3.1.3, it could be an excitation due to the presence of the 8 poles and 16 teeth at the input gear. Although the increase amplitude at order 16 amplitudes show a clear difference, other samples might be taken that are not as clear which could show not such drastic increase in terms of amplitude.

5.4 Dismantled Gearbox

After running the gearbox sufficiently enough to gather the information regarding its defect-free state, the decision is made to dismantle the gearbox to identify what defects are possible to be made. This process is made with the help of the Spindle Service Center in SKF Schweinfurt.



Figure 44 Dismantled Nabtesco RV-42N

5.5 Artificial Defects

After obtaining all the information regarding the possible defects of the gearbox and the bearings and the frequency response of each reported in section 5.2, the next step is the decision on what defects are to be made. It should be noted that not all defects are possible in this case due to the inability to dismantle the bearings from the shafts. The presence of the pinion outside the gearbox, easily accessible allowed the possibility to apply damages easier than of the gearbox's internal components. The first reported damage is simulated wear on the pinion and those that follow are on the gears and the bearings.

5.5.1 Pinion Wear

The pinion initially is in good condition, but with the usage of a small milling tool, it is possible to simulate some wear by chipping some of the teeth profiles. As reported in section 5.2.1, wear is noticeable as increase in sidebands around the GMF and in amplitude of the input frequency. Figure 45 reports the sensors from the pinion with wear to that without wear where, to show results from all sensors, the weight is removed, and the gearbox runs at constant speed.

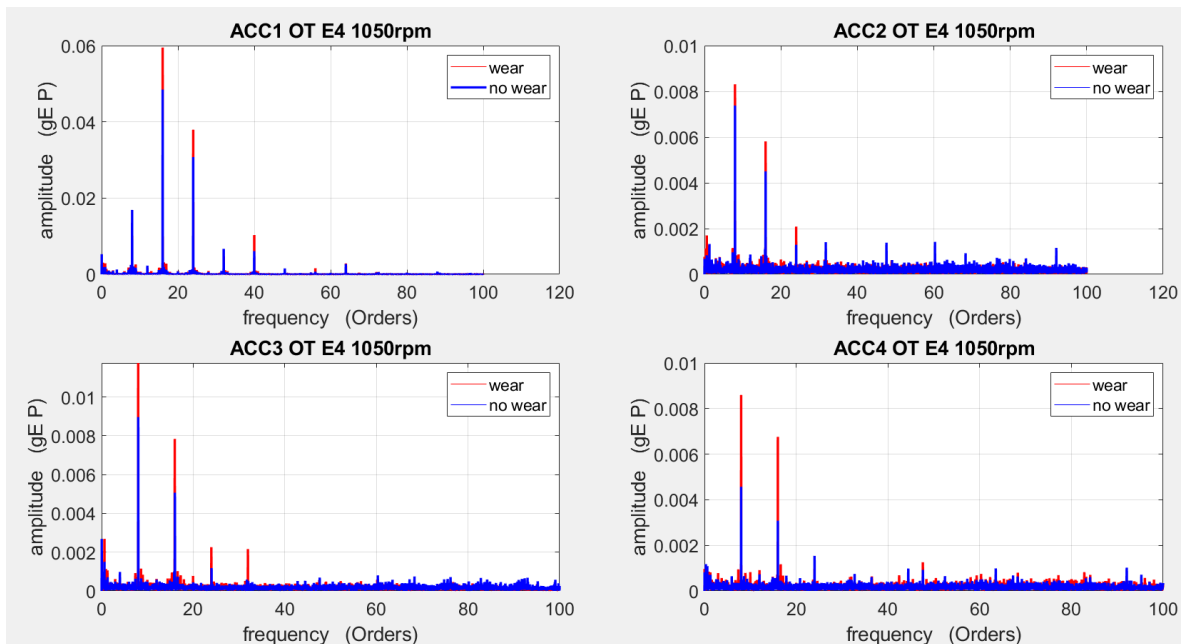


Figure 45 Difference in wear on input pinion, constant speed at 1050 rpm with Order Tracking and Envelope 4

5.5.2 ACBB, CRB and Disk Damage

After the acquisition of the results, the defected input pinion is removed, and a new pinion is put. The ability to place damages on many parts is the task to do keeping in mind to have them well spaced out in the frequency range. The list of damages made that shows a difference in the frequency spectrum and what they represent in terms of frequency response are listed in the table below.

Damage	Frequency response	Frequency modulation
ACBB inner ring	$0.135 * x$ (e.33)	New frequency rises
CRB outer ring	$1.8828 * x$ (e.34)	New frequency rises
Disk wear	-	Increase in amplitude of DMF and sidebands of GMF

Table 21 Frequency response to artificial Damages to Gearbox

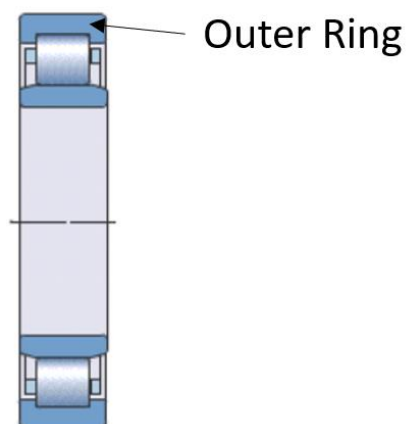


Figure 46 section view of CRB with outer ring specified (skf.com 2019)



Figure 47 Artificial damage to ACBB outer ring

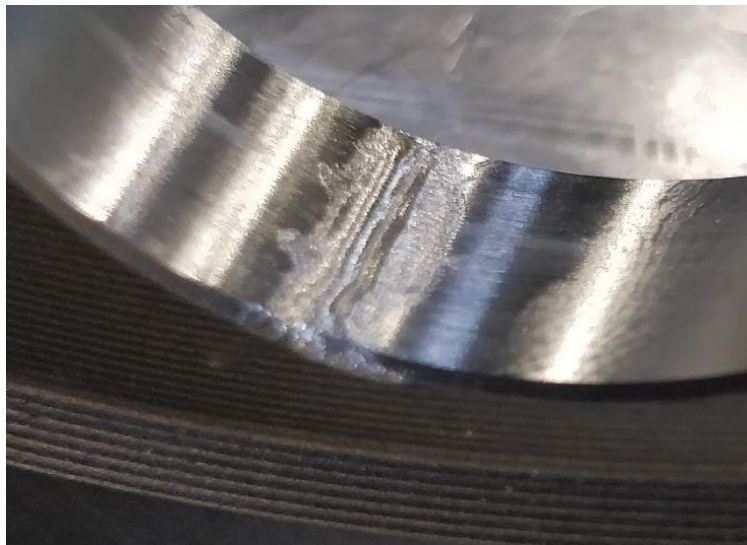


Figure 48 Artificial damage to the integrated CRB outer ring



Figure 49 Artificial Damage on to Disk undulations

After the damage is made, the disk is reassembled and put to run. Figure 50 reports the vibrations from the constant speed condition and figure 51 reports the robotic cycle condition.

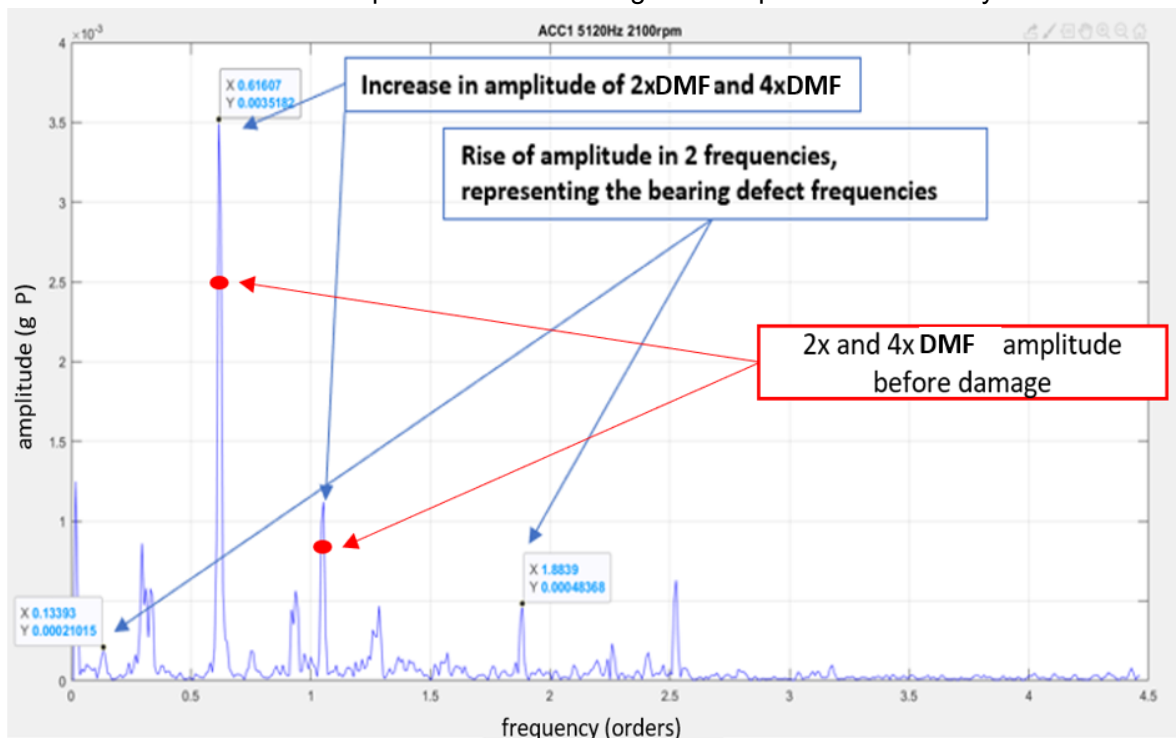


Figure 50 Damaged gearbox frequency response at constant speed of 2100 rpm

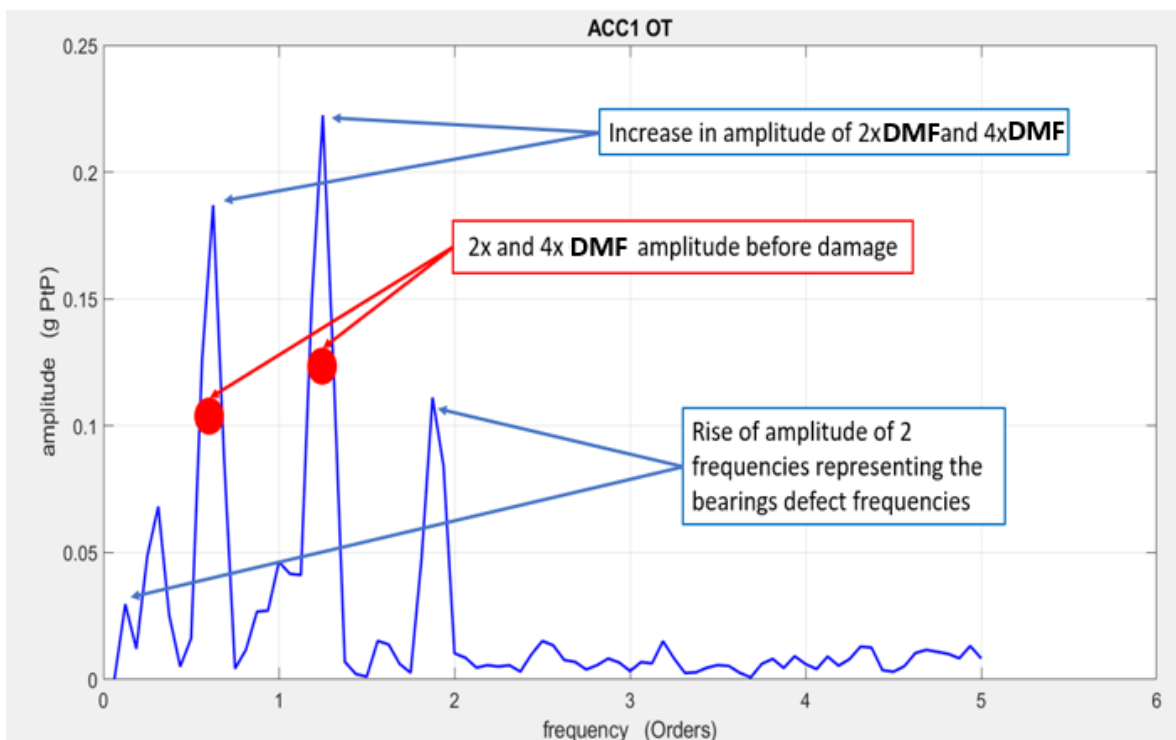


Figure 51 Damaged Gearbox with Order Tracking of raw data with robotic Cycle

Figure 51 reports the damaged gearbox in terms of frequency response up to 5 orders of the input frequency. The reason behind the reporting and interpretation of the raw signal is due to the inflicted damage onto the bearings where experts in the field expect to detect this type of artificial damage in the raw data domain since the filtering done by the enveloping would filter out this defect frequency.

5.5.3 Interpretation

The first defect of the pinion wear is reported in section 5.5.1 with figure 45 showing the difference this simulated wear has caused. It can be seen that the amplitude of the meshing has increased, in addition to the sidebands. The results can verify the wear present, although not big enough, which is expected to cause such signal modulation.

The other defects made and at this stage it is important to clarify that these defects have to be large enough to be noticed since previous smaller defects, seen in Appendix A.3, are made that do not cause a change to the spectra. Figure 50 reports the change in the frequency spectrum of the raw signal at constant speed where the 3 frequencies highlighted could represent the defects made. The first represents the damage made to the ACBB, the second is the increase in amplitude which is due to the disks and the third due to the CRB outer ring.

Figure 51 represent the order tracked signal of the damaged gearbox where the 16 revolutions initially setup are not sufficient to detect the damage and to have more accurate data, a second reflective tape is added onto the input. This doubled the resolution in terms of frequency spectra but gave less accurate measurement about the speed. The figure shows a rise to 2 frequencies previously not present; these represent the bearing defects since they are within the range of those frequencies in addition to an increase in the DMF's amplitude and harmonics.

5.6 Machine Learning - PCA

After the vibrational analysis section, machine learning and its possibilities in this area is reported in this section. Starting from the implementation where PCA is used then the interpretation where the data that are used are analyzed leading to the conclusion of this section.

5.6.1 Implementation

One of the first steps onto ML is the transfer of the Binning Algorithm onto KNIME. KNIME integrates various components for machine learning and data mining through its modular data pipelining concept. It contains the tools necessary to make anomaly detections and ML algorithms. [49]

This topic is addressed as the final stage of this work and is discussed with an expert in the field to know what is and could be possible to do. At this stage, the opportunity to perform a simple anomaly detection is possible with PCA explained in section 2.7.5 on data gathered from the non-defective gearbox and then test whether the algorithm is capable of differentiating the defective from those that are not. The difference is not only the defects themselves but also the difference between the grease inside each gearbox where the defective gearbox has grease with 4x higher viscosity. The model is built with 100 good data and 20 defective data. The process is made in KNIME, with its prebuilt PCA nodes and the workflow is shown in figure 52. The “Good” represents the gearbox with no defects and lower viscosity grease while “Damaged” or “Defective” represents the gearbox with the defects and 4x higher viscosity grease.

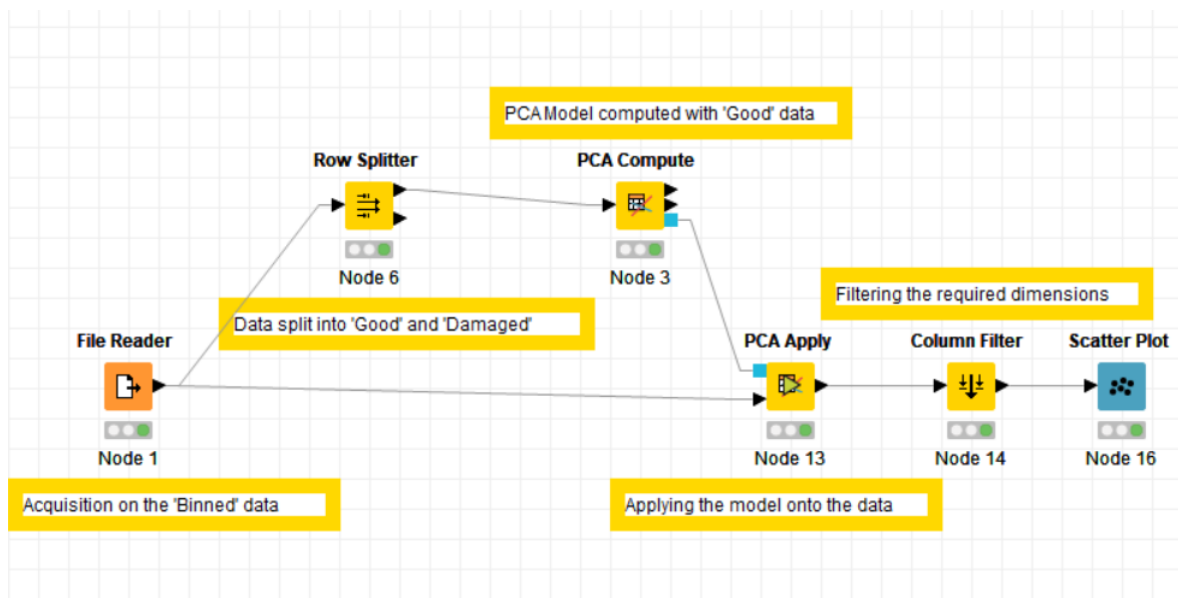


Figure 52 KNIME PCA workflow

To start off, the 120 gathered samples from the gearboxes are gathered in the same setup keeping in mind the difference in the greases' viscosity present between the two. The

acquisition of the data is done within the same day all from Acc1 with Envelope between 100Hz and 2000Hz done as post processing before passing through the Binning algorithm.

As this is an anomaly detection technique, the PCA model is built with the “Good” gearbox data. Then this model is passed through to apply it onto all the gathered data in order to show differences, if they exist. The next step is to plot the PCA dimensions and visualize the data points as is shown in figure 53.

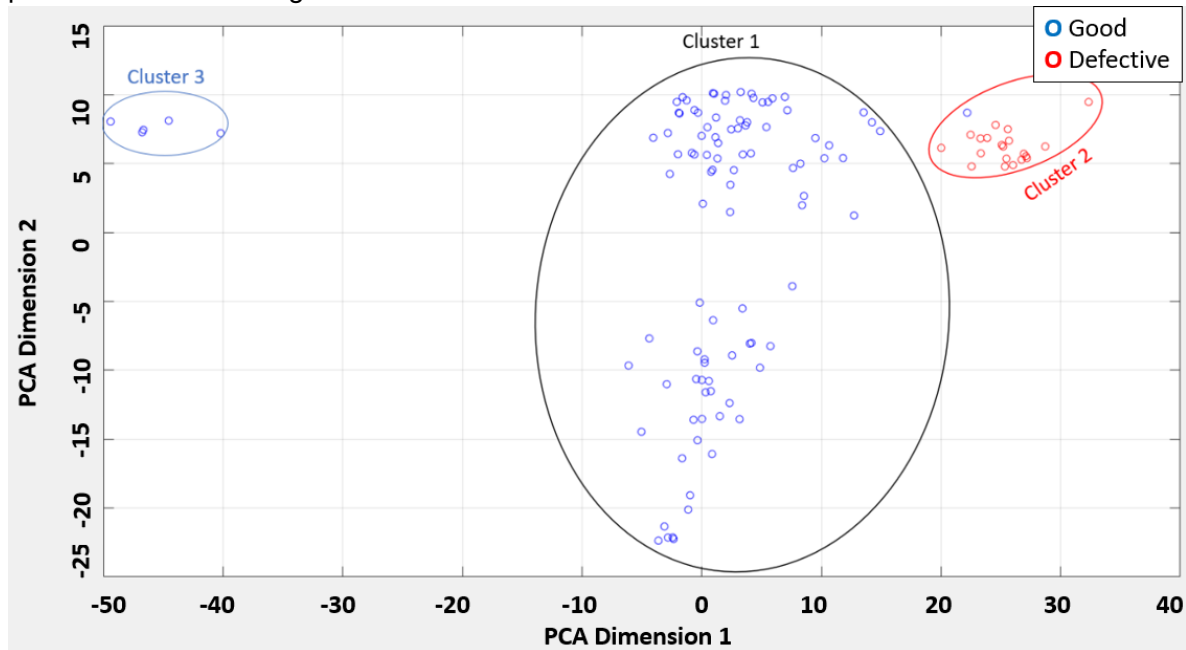


Figure 53 PCA output plot with model built with Good data

The reported figure shows clearly the presence of clusters with the biggest being Cluster 1 representing most of the “Good” gearbox data. Cluster 2 represents mostly the “Defective” gearbox data and cluster 3 represents some data points that are from the good gearbox. These initial results showed good separation, but they need to be clarified even more, especially cluster 3, in order to understand the differences.

5.6.2 Interpretation

In order to clarify the presence of the “Good” gearbox data of cluster 3 being far away from cluster 1, the data they represent is found in figure 54 and 55 below. Figure 54 represents 2 data points from Cluster 1 and 2 data points from Cluster 3. These data represent what is the input to the PCA model used in KNIME.

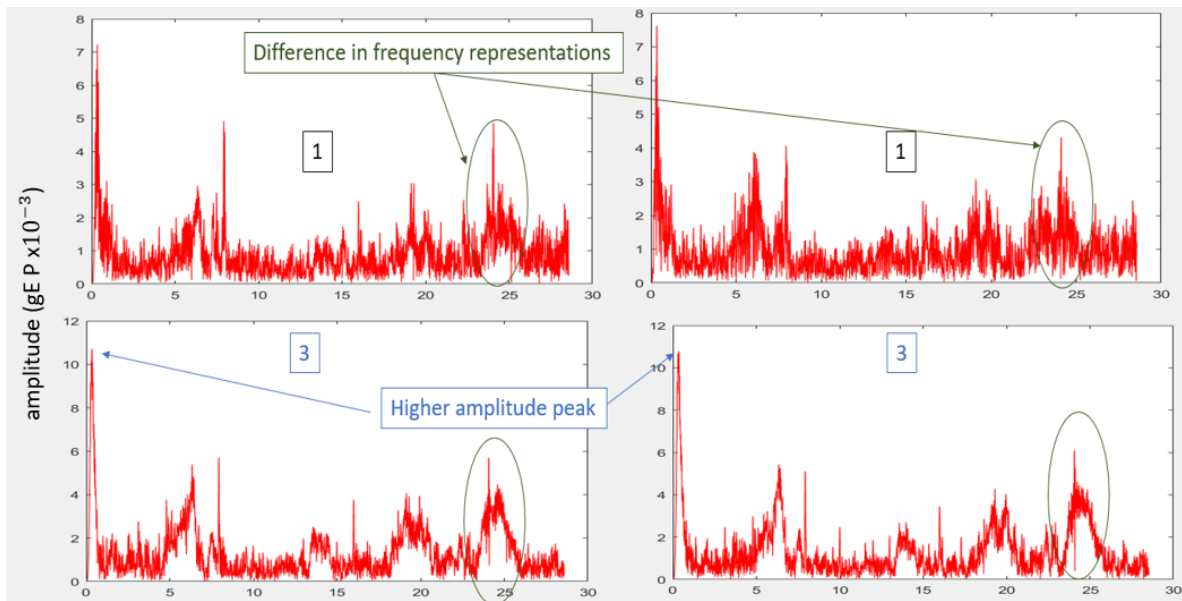


Figure 54 Data points from Cluster 1 and Cluster 3 in frequency spectrum (orders) after the Binning Algorithm

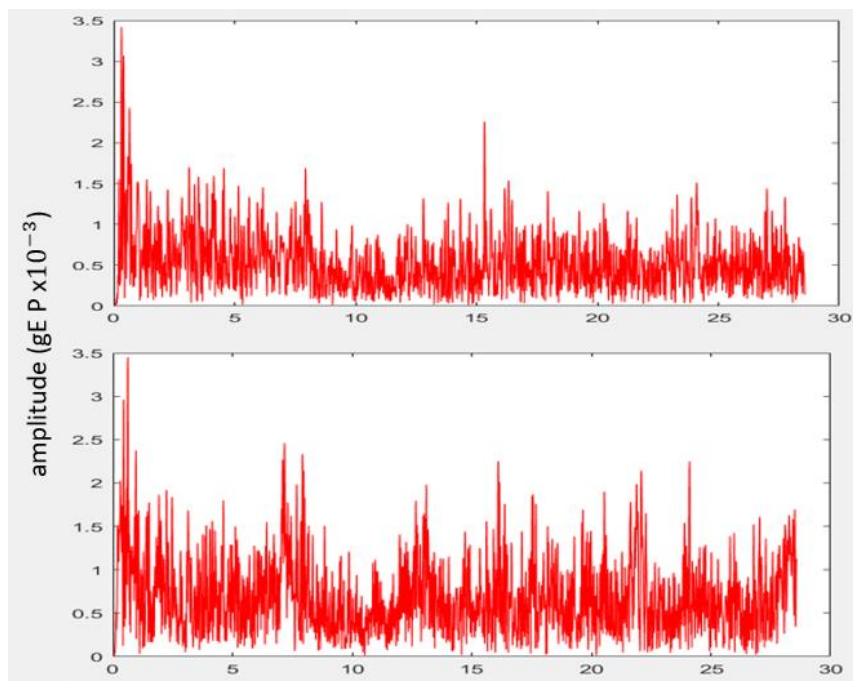


Figure 55 Data points from Cluster 2 in frequency spectrum (orders) after the Binning algorithm

As shown in the figure, the presence of higher amplitudes in Cluster 3 could be a reason for this separation. Another reason is the low amount of vibrational data that are used for the Binning algorithm for the data points in Cluster 3. This is visible where the spacing between one frequency measurement and another is higher than that of Cluster 1 where only the first section of the cycle is taken. Regarding Defect Data measurements and specifically Cluster 2, the frequency representation from the Binning algorithm is represented in figure 55. Figure 55 shows a big difference in terms of amplitude peaks from those of Cluster 1 and 3. In addition to that, the frequency spectrum is not as clear where the peaks at order 16 or 8 have sidebands with high amplitude in addition to harmonics of the input speed.

5.6.3 Conclusion

Starting with the difference between the good data in Cluster 1 and Cluster 3, the most probable reason between the separation is the higher amplitude that is present throughout the spectrum. Since the data are passed first through the Binning algorithm, the amplitude modulation that is done increased the amplitude in presence of low sample size. This correlates well with the separation that is done between the “Good” gearbox data and the “Defective” gearbox where also in that case we have an amplitude difference throughout the spectrum. Although the difference between Clusters 1 and 2, the “Defective” and “Good” gearbox, can be related to amplitude values, the algorithm is capable of separating them as shown clearly in figure 53. The amplitude difference most probably goes back to the difference in grease between the two rather than actual defects. The knowledge of the grease of the “Defective” being 4x more viscous than the “Good” and visualizing the difference amplitudes as shown in figure 54 further enforces that suggestion. Although a separation is made, it is most likely that the grease is the reason which then makes this based on grease rather than defects. In terms of anomaly detection, the objective is reached due to the separation of 2 gearboxes.

The data and the result show positive results of what could be possible in this field in the future, but this is just a preliminary result. Further investigation onto this field should be made with more data and more complex algorithms. Now that the final step is done, the next chapter briefly summarizes the whole work and then discuss what could be possible for future work.

6. Conclusion

In robotics, it doesn't exist yet a commercially available technique that is possible to detect defect in robots during their normal working conditions. Knowing that a defect occurs within a robot a long time before actual failure, this work was done on vibration monitoring of a robotic gearbox in order to test the possibility of detection.

The work started with the kinematic study of a robotic gearbox, Nabtesco RV 42-N, to understand the vibration frequencies that it emits during motion. This study was the bases of which all frequencies, defective and non-defective, in order to differ a defective gearbox from one at good condition. The operating condition for the gearbox was either at constant speed or a robotic cycle.

Signal processing methods used during this work were the raw data, enveloped, order tracked, Matlab's Envspectrum and the SKF Binning algorithm. The work has shown a positive result for the SKF Binning algorithm where this work was a first stage in testing its quality. Enveloping was used and the E4 has shown to give the best results in terms of meshing of the gears in its 2 stages. In addition, Order tracking showed better results than the Binning considering the defects made.

Several artificial defects were made, the defects' frequencies were visible with the methods used in terms of constant speed and with the cycle. Wear on the gears would increase the amplitude of the meshing and that was shown. Bearing defect frequencies should rise after a damage was made and that was shown for the ACBB and the CRB of this gearbox.

ML was tested, and the result shows a clear cluster differentiation between 2 gearboxes most probably related to difference in grease. However, the results were preliminary and needs more comprehension in addition to more data.

This work shows a positive result in vibration monitoring of a robotic gearbox which could be a first step in further investigations and work. The non-cyclostationary operation conditions of robotics has always been a challenge, but with proper tools, this work has shown the possibility of defect detection.

7. Future Work

The work done and the results could provoke other work in this field, and if so, a chapter discussing what can be done to improve the results is done here. Although other similar setups can be made, some improvements can be seen and done in the future. First, the setup needs to be evaluated and how it can be improved in terms of the test rig and the acquisition system. Then a discussion for other fault detection methods and signal processing techniques in vibration monitoring could be done as well as ML.

7.1 Test setup improvements

The test rig setup has been explained in chapter 4 from the actual structure of the setup up to the signal acquisition kit and the software implementation. The utilization of mostly SKF equipment is helpful in further understanding the tools as in the sensors and the *SKF Multilog™ On-line System IMx-8* with the interface *SKF @ptitude™ Observer*. Table 21 reports the equipment of the setup and possible improvements.

Equipment	Status	Evaluation
<i>SKF Multilog™ On-line System IMx-8</i>	Increase acquisition time for high frequency sampling for post processing techniques	Sufficient
<i>SKF @ptitude™ Observer</i>	Outputs data in numerous modes	Sufficient
Test rig structure	Requires to be fixed in all directions	Needs improvement
Sensor placement	Placed as close as possible	Sufficient
Accelerometers	Good frequency range	Sufficient
Tachometer	Utilization of inductive tachometer for better order tracking results	Needs improvement
Noise isolation mats	Showed very good isolation	Sufficient

Table 22 Test setup Improvements

Now that all the setup components have been reported, another improvement could be to have a new gearbox and let it run until a defect through vibration analysis is detected. Rather than waiting for the failure to occur, stopping and dismantling the gearbox to verify the data could be highly valuable. It would correlate the stage of defect damage to the data and further down the line predict the life left in the gearbox with the amplitude of the signals.

7.2 Other Methods

During this work, the focus was on CBM using vibration signals, however, there are other methods that could yield a good result as well. First will be discussed other methods and the possibility of other signal processing techniques. The methods to be reported could be of value in combination with vibration analysis to further verify what is the current state of the monitored asset.

7.2.1 Defect Detection Methods

In addition to vibration analysis, there are methods that could be valuable to discuss as in acoustic emission and current signal analysis. Both these methods have several papers done and can be found to be successful in detecting defects for rotary equipment. Their presence however in robotic gearboxes and their complexity could be a drawback but their inclusion in this chapter is worthy.

7.2.1.1 Acoustic Emission

Acoustic Emission was first developed for testing static structures, but it has been extended into the field of health monitoring of rotary equipment. [50] The emissions are emitted when a material has irreversible changes to its structure and when it undergoes load, the waves are emitted. The emission propagates through the whole structure which is good in terms of position for the sensor, but defect signal would carry other unwanted signals and would require specific filtering.

Regardless of the implementation complexity, this method has been tested and proven to have a positive result in detecting defects especially in bearings. A research work [50] has been done with the aim of detecting a bearing defect on a radially loaded bearing. The system was set with the purpose of having high noise and this method was capable of detecting the defects. Another research, [51], was made on a gearbox with defect on bevel gears inside it having the sensor as close as possible. These results show the possibility of such implementation in the field of robotic gearbox monitoring.

7.2.1.2 Motor Current Signal Analysis

Another method to discuss is the Motor Current Signal Analysis, it studies the current of the motor at steady state and its variation in order to detect defects. This method could be used alongside the vibration monitoring to verify the results of both. A research work using both these methods has been done, see [52], and proved that for each an advantage in detecting faults within a motor. Although it specifically aims towards the motor condition, it can also be used to detect defects in a gearbox, since that as well would modulate the current signal.

7.2.2 Signal Processing techniques

This work has shown the possibility of using the SKF Binning algorithm in detecting the normal working condition of a gearbox and thus verify its quality. However, several signal processing techniques exist and have been mentioned throughout the literature study, and the presence of the enveloping method shows good results. Knowing that the bearings' rolling elements cause excitations in presence of defects, the enveloping method is capable of differentiating those and keeping the defect frequencies. The enhancement in this area could be to have smaller enveloping frequency ranges specifically designed for the asset monitored which would amplify the specific responses of the bearings themselves.

Regarding the gears, using the E4 has shown to keep the meshing frequencies and negate the others. This is useful to have especially during trend analysis of an actual gearbox in operation,

where the frequencies will be monitored and through an increase in amplitude, a defect could be detected. In addition to the available enveloping techniques, an E5 would be a good addition to this field. This envelope would be useful to have since an E4 was able to filter out all the other signals but an E5 might even give better results considering gears meshing.

An important tool to mention is the acquisition and storage on raw data where in presence of a technique to be tested, it can be done on those data and evaluate if the technique is better than what has been already done. Regarding other signal processing techniques, a technique that would be of benefit is the spectral Kurtosis.

7.2.2.1 Spectral Kurtosis (SK)

SK is a statistical tool which can indicate the presence of series of transients and their locations in the frequency domain. [53]. This tool could be of value in terms of detecting defects in the non-cyclostationary conditions. A research paper has been published regarding its usefulness in the field of Vibration Condition Monitoring showing its capabilities, see [54]. This method, however, needs accurate filtering techniques as enveloping to be designed for the fault to be detected. Although this technique seems to be complex, the research paper has shown on actual cases its usefulness in rotating machines making it an interesting method to be studied.

7.2.3 ML

This work shows a positive result in differentiating 2 gearboxes, a new gearbox and a defected one with much thicker grease using supervised anomaly detection specifically PCA. An expert in the field of ML, Dr. Lukas Koeping, suggests that the next step in this field should be taken and it would be to use one class SVM, Support Vector Machine. The results of this could promote other methods as well including unsupervised methods which could give better results. In addition to this, the data gathered should be held on to and be used in testing other methods. This complex field, ML, could lead to have a technique capable of not only identifying a damaged gearbox but it could also identify the specific defect.

8. Bibliography

- [1] scanimetrics, "scanimetrics.com," Scanimetrics Inc., [Online]. Available: <https://www.scanimetrics.com/index.php/scanimetrics-news-menu-item/10-equipment-monitoring/98-equipment-condition-monitoring-a-history>.
- [2] G. Erboz, "HOW TO DEFINE INDUSTRY 4.0: The Main Pillars of Industry 4.0," Gödöllő.
- [3] S. Group, "SKF - about SKF," SKF Group, 2019. [Online]. Available: <https://www.skf.com/de/our-company/index.html>. [Accessed 10 October 2019].
- [4] S. Group, "SKF.com," 2018. [Online]. Available: <https://www.skf.com/binaries/315-455097/0901d196807fe195-REP-brochure---18072-EN.pdf>. [Accessed 10 October 2019].
- [5] "UPGRADE AT SMURFIT KAPPA," SKF Evolution Magazine, Thursday 6 December 2018.
- [6] I. O. f. Standarization, "ISO 8373:2012 Robots and robotic devices - Vocabulary," ISO/TC 299 Robotics Technical Committee, 2012.
- [7] L. Deinhofer, "Training Package 1- Overview and introduction," SKF internal Document, 2019.
- [8] M. Budimir, "motion control tips," 4 August 2017. [Online]. Available: <https://www.motioncontroltips.com/what-is-a-gearbox/>. [Accessed 10 October 2019].
- [9] L. Deinhofer, "Package 4 Compact Gearbox in Robotics," SKF internal document, 2019.
- [10] Nabtesco, "Nabtesco," [Online]. Available: https://www.nabtesco.com/en/library/annual_report/oar2012/overview/at_a_glance.html.
- [11] "wikipedia," wikipedia, 21 October 2019. [Online]. Available: [https://en.wikipedia.org/wiki/Bearing_\(mechanical\)](https://en.wikipedia.org/wiki/Bearing_(mechanical)). [Accessed 30 October 2019].
- [12] SKF, "SKF," SKF group, 2019. [Online]. Available: <https://www.skf.com/sg/products/bearings-units-housings/ball-bearings/angular-contact-ball-bearings>. [Accessed 30 October 2019].
- [13] SKF, "SKF.com," [Online]. Available: <https://www.skf.com/ca/en/products/bearings-units-housings/ball-bearings/angular-contact-ball-bearings/index.html>.
- [14] S. group, "SKF," SKF Group, 2019. [Online]. Available: <https://www.skf.com/uk/products/rolling-bearings>. [Accessed 30 October 2019].
- [15] C. Gonzalez, *What's the Difference Between Bearings?*, 2015.
- [16] S. R. B. Catalogue, "SKF.com," [Online]. Available: <https://www.skf.com/binary/21-121486/Rolling-bearings---17000-EN.pdf>.
- [17] F. Porzio, "VIB 1_rev3_2018," SKF internal document, 2018.
- [18] Dave, "watelectrical," 29 March 2019. [Online]. Available: <https://www.watelectrical.com/6-different-types-of-temperature-sensors-with-their-specifications/>. [Accessed 30 October 2019].
- [19] M. Dhiman, "slideshare," 2 November 2015. [Online]. Available: <https://de.slideshare.net/Manishd94/velocity-sensors-inrobotics>. [Accessed 30 October 2019].

- [20] B. Å. L. v. S. Hugo Jan Alrik Danielson, "Robot Condition Monitoring," Luleå University of Technology , 2017.
- [21] F. H. Martin Karlsson, "Robot Condition Monitoring and Production Simulation," Luleå tekniska universitet, 2018.
- [22] S. G.K. and A. S. Al Kazzaz, "Induction machine drive condition monitoring and diagnostic research," Electric Power Systems Research, 2002.
- [23] "inspectioneeing.com," [Online]. Available: <https://inspectioneeing.com/tag/condition+based+monitoring>.
- [24] R. B. Randall, Vibration Based Condition Monitoring, Wiley, 2011.
- [25] M. -. Gearbox, "Mobius Institute - Broken tooth," Mobius Institute, 2019. [Online]. Available: <https://www.mobiusinstitute.com/site2/item.asp?LinkID=8061&iVibe=1&sTitle=Gearbox>. [Accessed 10 October 2019].
- [26] "dataphysics.com," [Online]. Available: <http://www.dataphysics.com/applications/rotating-machinery-diagnostics/order-analysis-order-tracking-and-filtered-orders.html>.
- [27] J. Kolerus, in *Zustandsüberwachung von Maschinen*, Renningen-Malmsheim, 2000.
- [28] "Ni Instruments - Understanding FFTs and windowing," 2019. [Online]. Available: <http://download.ni.com/evaluation/pxi/Understanding%20FFTs%20and%20Windowing.pdf>. [Accessed October 2019].
- [29] L. -. m. university, "https://www.uni-muenchen.de/index.html," LMU, [Online]. Available: https://www.phonetik.uni-muenchen.de/~jmh/lehre/Rdf/EMU-SDMS/lesson9/09_Spectral_analysis.html. [Accessed 08 October 2019].
- [30] A. Fernandez, "power mi," [Online]. Available: <http://www.power-mi.com/content/demodulation-or-envelope-analysis>. [Accessed 08 October 2019].
- [31] C. Instruments, "crystalinstruments.squarespace.com," [Online]. Available: <https://static1.squarespace.com/static/5230e9f8e4b06ab69d1d8068/t/56d5e7e3b09f9563dd2ffe5b/1456859108792/Introduction+of+Time+Synchronous+Averaging.pdf>.
- [32] Slawik, Verena, "Development of a cindition based monitoring concept for high reduction ratio gearing (Analysis part : Blinning)- Internal Report," SKF, Schweinfurt, 2017.
- [33] N. Y. H. N. S. D. Y. M. M. N. M.C. Isaa, "Ferrogaphic Analysis of Wear Particles of Various Machinery Systems of a Commercial Marine Ship," *Procedia Engineering* , vol. 68, pp. 345-351, 2013.
- [34] "expertsystem.com," 7 March 2017. [Online]. Available: <https://expertsystem.com/machine-learning-definition/>. [Accessed 08 October 2019].
- [35] S. Z. B. W. T. G. H. Shen Zhang, "Machine Learning and Deep Learning Algorithms for Bearing Fault Diagnostics – A Comprehensive Review," 2019.
- [36] I. K. Andrzej Puchalski, "Data-driven monitoring of the gearbox using multifractal analysis and machine learning methods," in *MATEC Web of Conferences* 252, 2019.
- [37] Y. Z. L. D. J. X. L. Z. Jinjiang Wang, "Virtual sensing for gearbox condition monitoring based on extreme learning machine," *Journal of Vibroengineering*, vol. 19, no. 2, pp. 1000-1013, 2017.
- [38] M. S. P. K. K. I. R. T Praveenkumara, "Fault diagnosis of automobile gearbox based on machine learning techniques," *Procedia Engineering*, vol. 97, pp. 2092-2098, 2014.

- [39] aishwarya.27, "geeksforgeeks.org," [Online]. Available: <https://www.geeksforgeeks.org/ml-principal-component-analysispca/>. [Accessed 08 October 2019].
- [40] "Matlab," Matlab, 2017. [Online]. Available: <https://fr.mathworks.com/help/signal/ref/envspectrum.html>. [Accessed 09 October 2019].
- [41] "Fabreeka," Fabreeka, [Online]. Available: <https://www.fabreeka.com/products/fabcel-nitrile-pad-vibration-isolation/>. [Accessed 09 October 2019].
- [42] Nabtesco, "RV series technical data," 2019. [Online]. Available: <https://www.nabtescomotioncontrol.com/pdfs/RVseries.pdf>. [Accessed 30 09 2019].
- [43] H. W.Muller, Die Umlaufgetriebe, Berlin: Springer, 1997.
- [44] M. -. Gearbox, "mobius institute - tooth load," Mobius Institute, 2019. [Online]. Available: <https://www.mobiusinstitute.com/site2/item.asp?LinkID=8057&iVibe=1&sTitle=Gearbox>. [Accessed 10 October 2019].
- [45] A. Fernandez, "https://power-mi.com/," 11 April 2017. [Online]. Available: <https://power-mi.com/content/frequencies-gear-assembly>.
- [46] A. Fernandez, "Power Mi," Power Mi, 27 February 2017. [Online]. Available: <http://www.power-mi.com/content/looseness>. [Accessed 10 October 2019].
- [47] "Vibration School," Vibration School, [Online]. Available: <http://www.vibrationschool.com/mans/SpecInter/SpecInter47.htm>. [Accessed 10 October 2019].
- [48] P. v. D. G. A. D. V. v. R. M. S. J. S. T. Gerrit van Nijen, Noise and vibration in bearing systems [2nd Edition], SKF Research & Technology Development, 2017.
- [49] KNIME, "KNIME About," KNIME, 2019. [Online]. Available: <https://www.knime.com/about>. [Accessed 31 October 2019].
- [50] D. M. A. Morhain, "Bearing defect diagnosis and acoustic emission," *Journal of Engineering Tribology* , vol. 217, no. 4, pp. 257-272, 2003.
- [51] D. O. W. H. a. A. T. Lu Zhang, "Acoustic Emission Signatures of Fatigue Damage in Idealized Bevel Gear Spline for Localized Sensing," *MDPI*, no. 7, p. 242, 2017.
- [52] J. A.-D. P. Popaleny, "Electric Motors Condition Monitoring Using Currents and Vibrations Analyses," in *XXIIIrd International Conference on Electrical Machines*, Alexandroupoli, GREECE, 2018.
- [53] Jérôme Antoni, "The spectral kurtosis: a useful tool for characterising non-stationary signals," *Mechanical Systems and Signal Processing*, vol. 20, no. 2, pp. 282-307, 2006.
- [54] R. Jérôme Antoni, "The spectral kurtosis: application to the vibratory surveillance and diagnostics of rotating machines," *Mechanical Systems and Signal Processing*, vol. 20, no. 2, pp. 308-331, 2006.
- [55] R.ABB, " "User guide and robot specification", " [Online]. Available: https://library.e.abb.com/public/560fa420555c2d8ac1257b4b0052112c/3HAC023933-001_rev1_en.pdf. [Accessed 27 09 2019].
- [56] "College Outreach Program Ball Bearing," SKF internal document, 2019.

9. Appendix

A.1. Frequency spectrum with and without weight

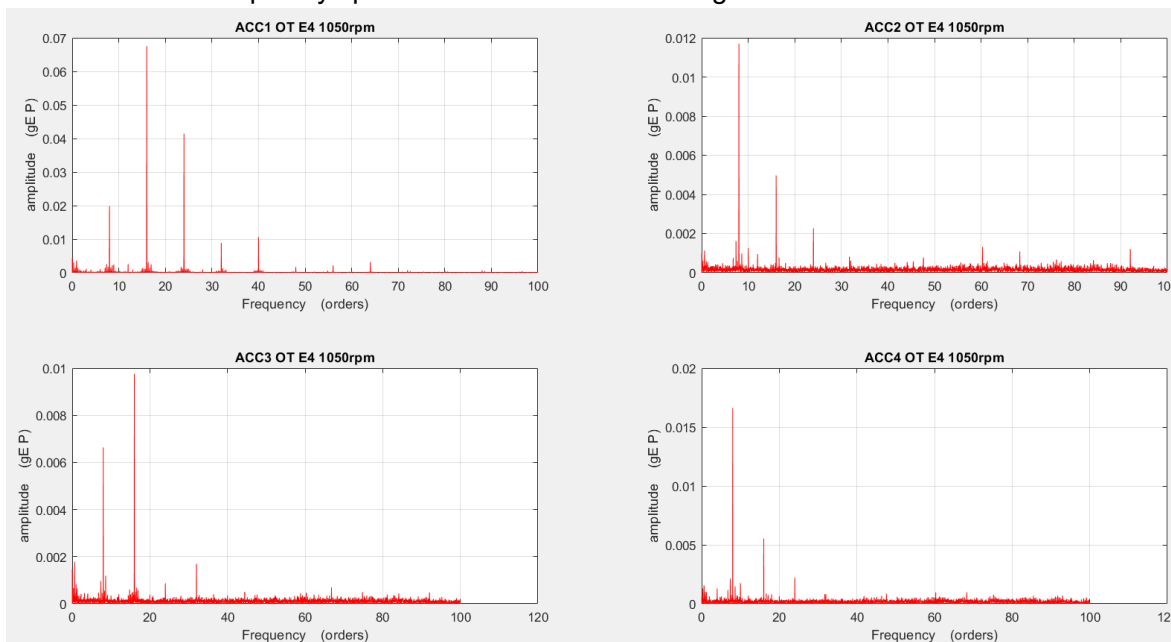


Figure 56 all accelerometers with OT and E4 at constant speed of 1050 rpm without added weight

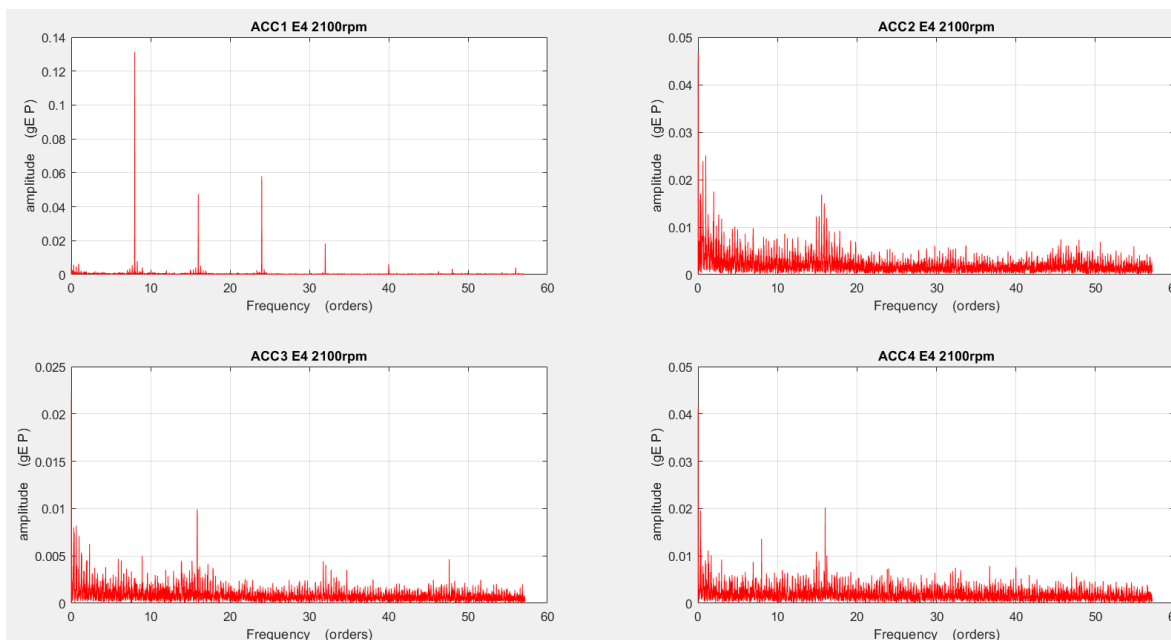


Figure 57 all accelerometers with OT and E4 at constant speed of 2100 rpm with added weight

A.2. Difference between enveloping, raw and Envspectrum at constant speed

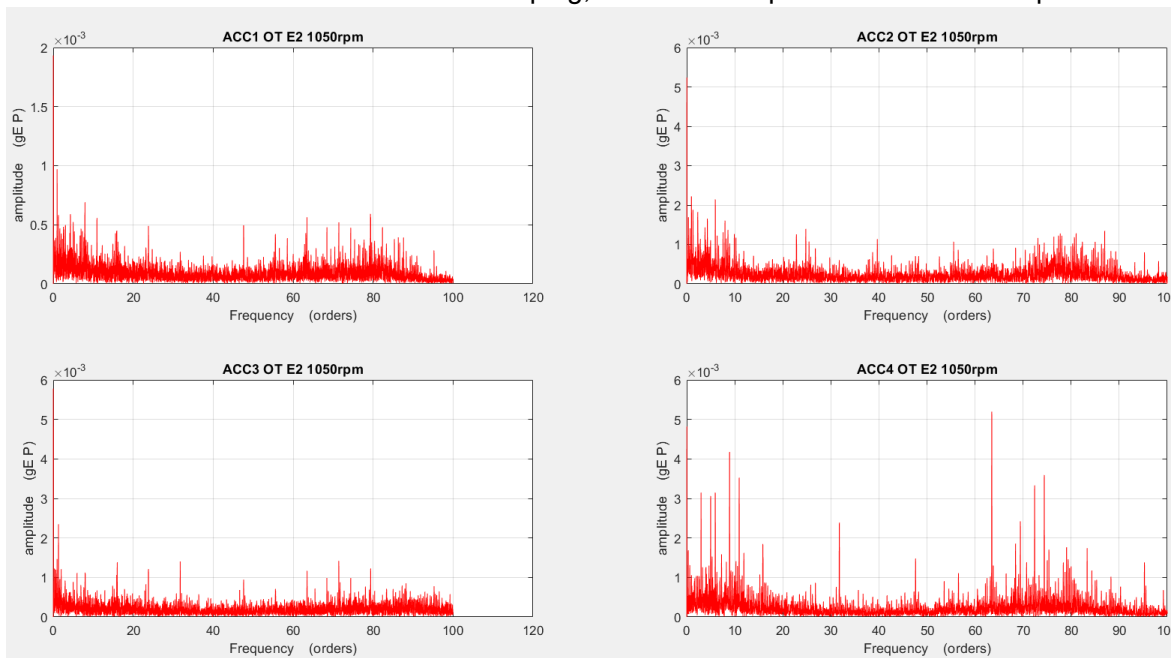


Figure 58 all accelerometers with OT and E2 at constant speed of 1050 rpm

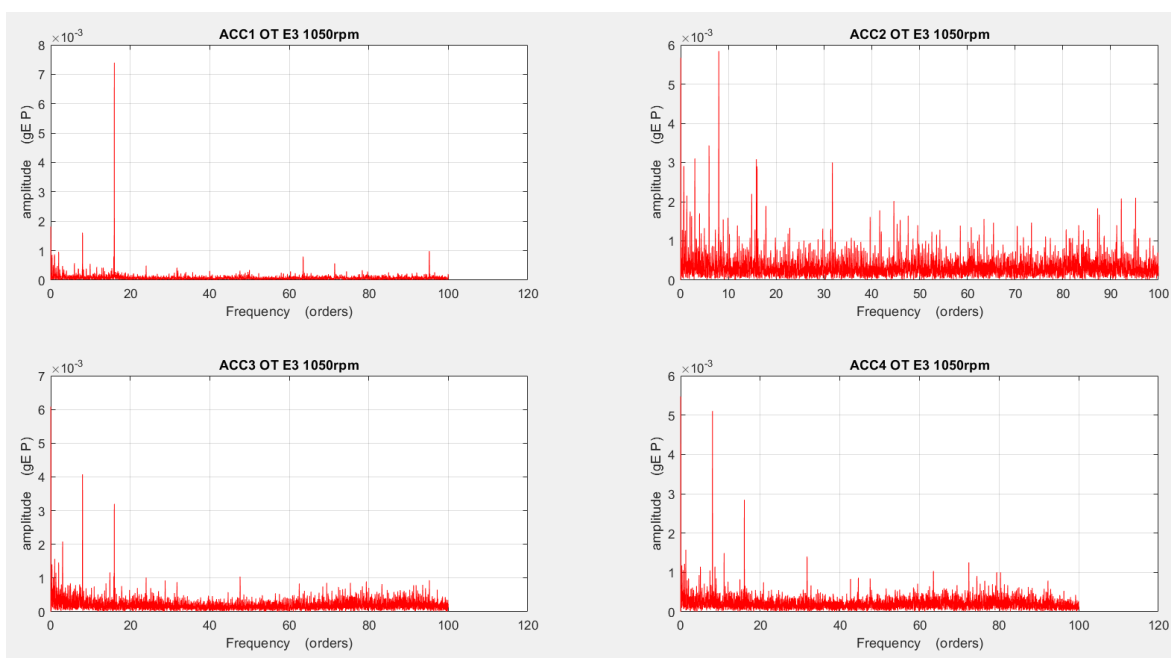


Figure 59 all accelerometers with OT and E3 at constant speed of 1050 rpm

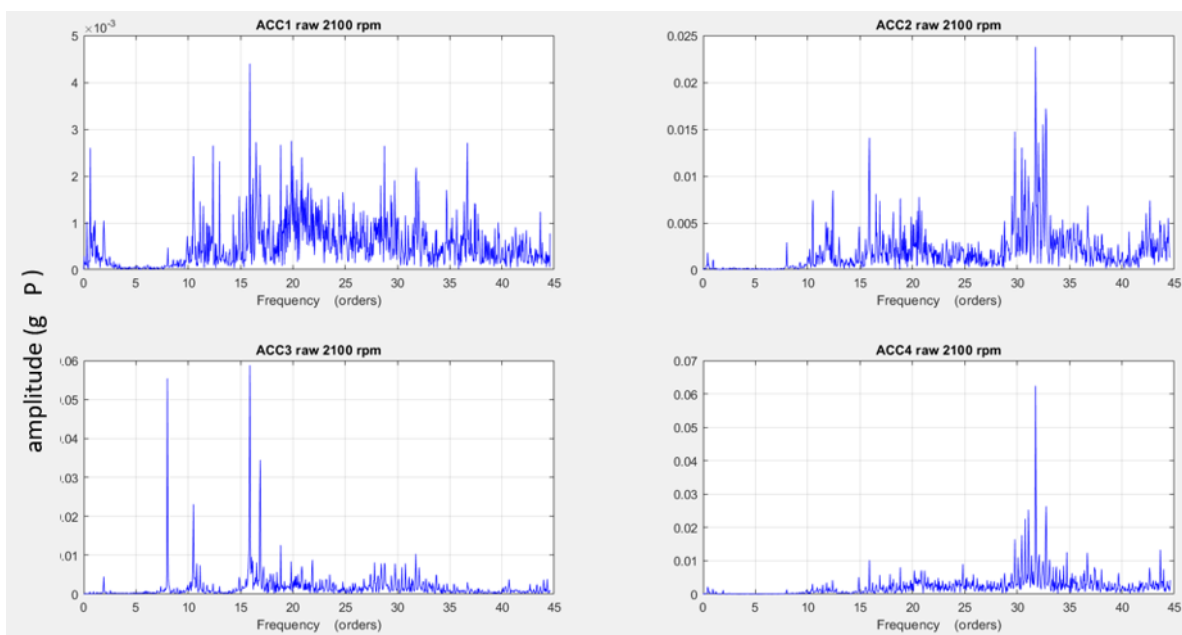


Figure 60 all sensors, raw data at constant speed of 2100 rpm

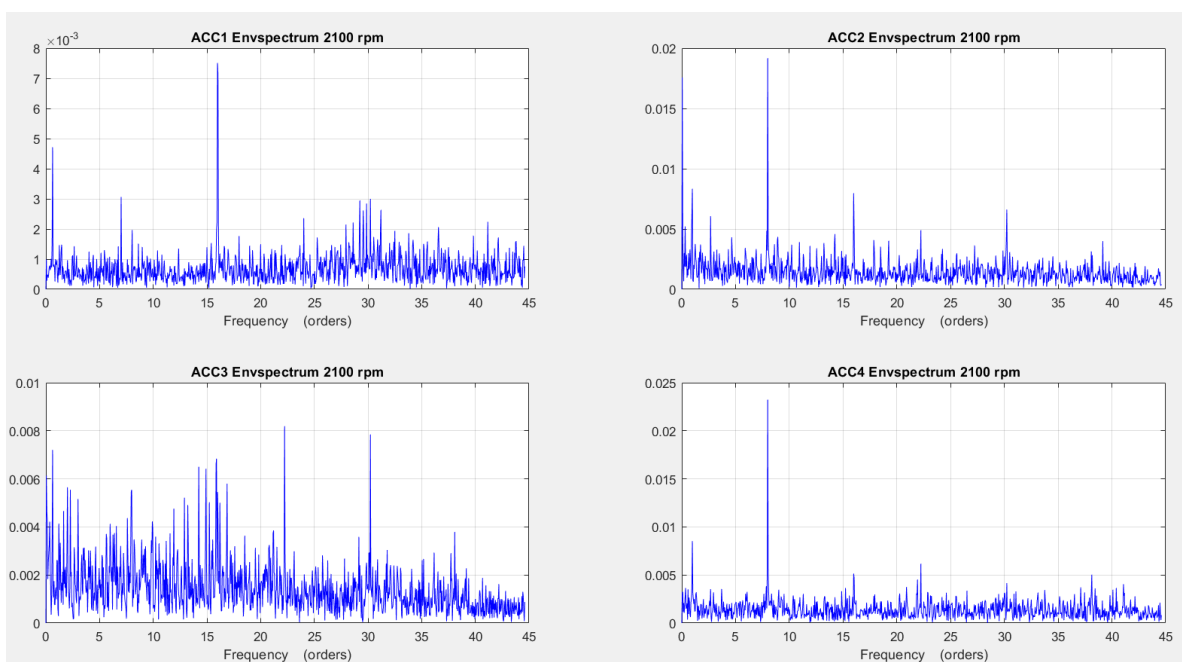


Figure 61 all sensors with Envspectrum at constant speed of 2100 rpm with amplitude as overall RMS

A.3. Initial Damages

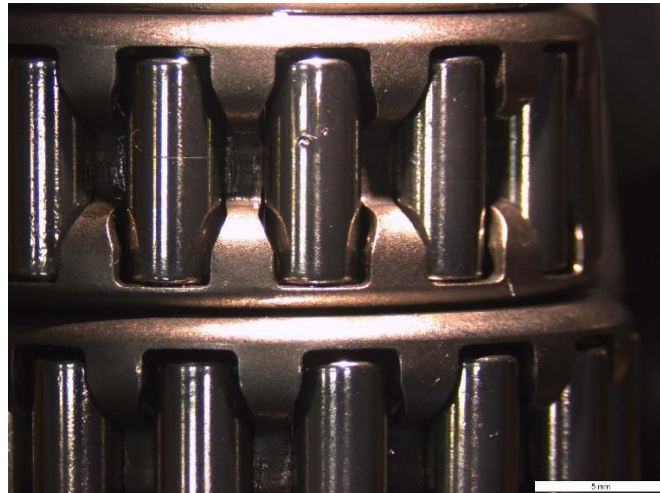


Figure 62 Initial Damage on CRB rollers



Figure 63 Initial Damage on the integrated CRB outer ring



Figure 64 Initial Damage on ACBB outer ring

A.4. Test Rig photos



Figure 65 Test rig feet with isolation mats

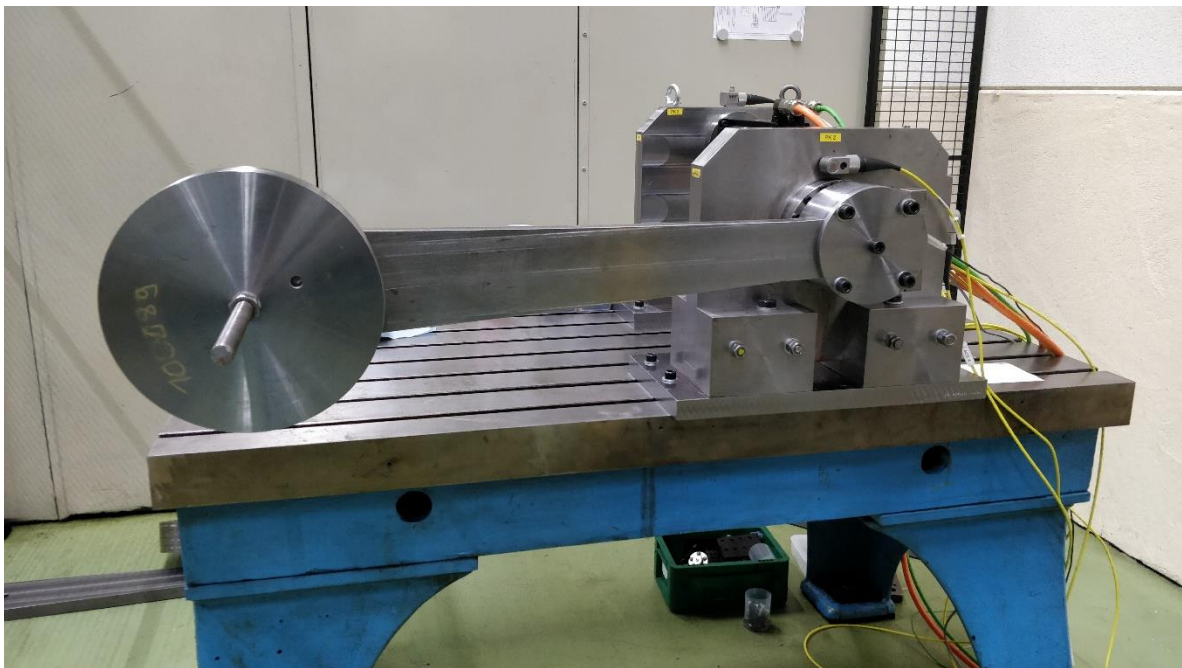


Figure 66 Test rig in initial position

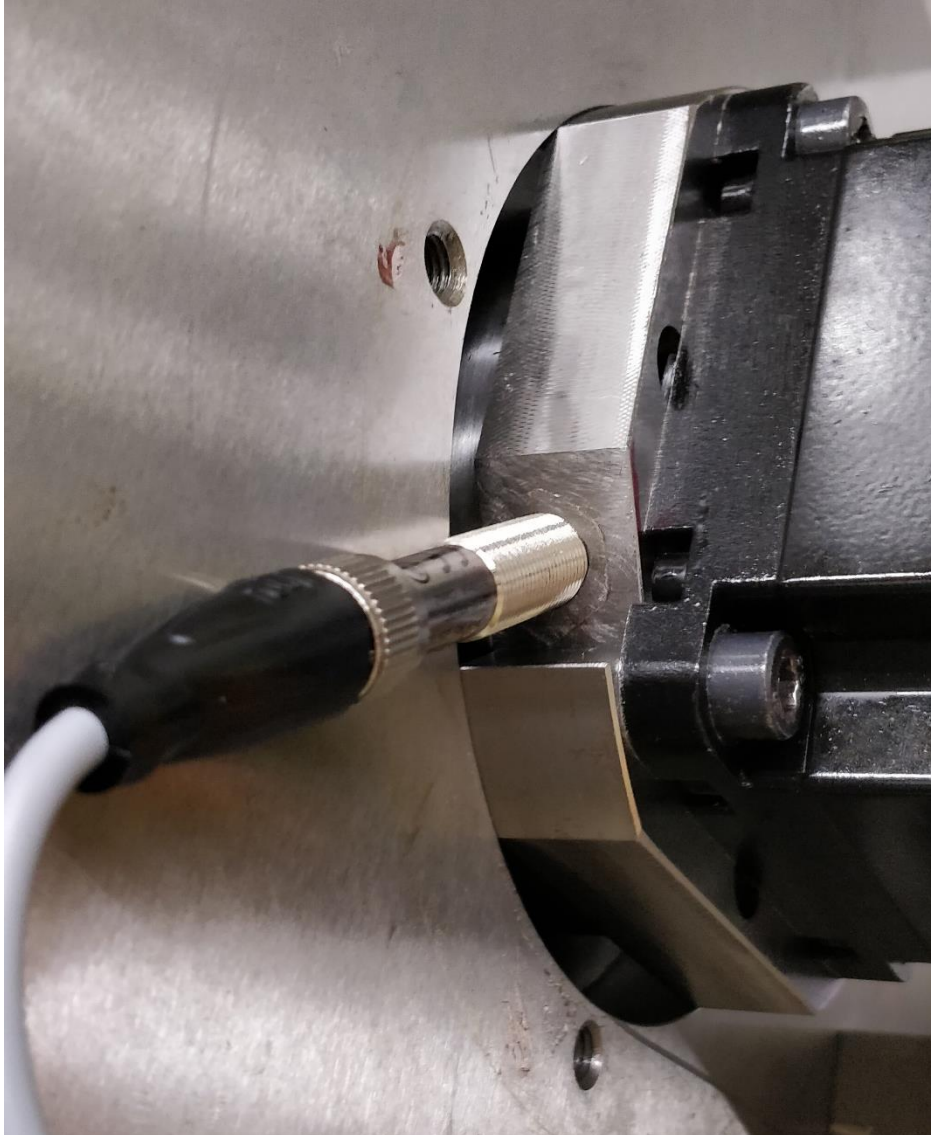


Figure 67 Tachometer placement at input side

A.5. Accelerometer and Tachometer Technical specifications

Specifications

Specifications conform to ISA-RP-37.2 (1-64) and are typical values referenced at 24 °C (75 °F), 24 V DC supply, 4 mA constant current and 100 Hz.

Dynamic

- Sensitivity: 100 mV/g
- Sensitivity precision: $\pm 10\%$ at 25 °C (75 °F)
- Acceleration range: 80 g peak
- Amplitude linearity: 1%
- Frequency range:
 - $\pm 10\%$: 1,0 to 5 000 Hz
 - ± 3 dB: 0,7 to 10 000 Hz
- Resonance frequency, mounted, minimum: 22 kHz
- Transverse sensitivity: $\leq 5\%$ of axial
- Temperature response: See graph

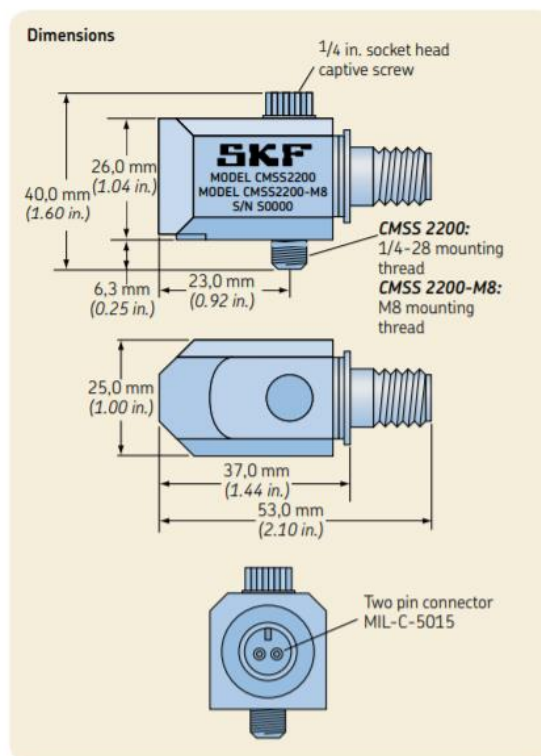


Figure 68 Accelerometer CMS 2200 specifications

Technical data		
General specifications		
Effective detection range		0 ... 2500 mm
Reflector distance		50 ... 2500 mm
Threshold detection range		3000 mm
Reference target		H50 reflector
Light source		LED, 640 nm
Polarization filter		yes
Angle deviation		+/- 2 °
Diameter of the light spot		approx. 150 mm at a distance of 2500 mm
Angle of divergence		approx. 3.5 °
Optical face		frontal
Ambient light limit		EN 60947-5-2 20000 Lux
Functional safety related parameters		
MTTF _d		800 a
Mission Time (T _M)		20 a
Diagnostic Coverage (DC)		0 %
Indicators/operating means		
Operation indicator		LED green: Power on
Function indicator		LED yellow: lights up when receiving the light beam ; flashes when falling short of the stability control; OFF when light beam is interrupted
Control elements		sensitivity adjustment
Electrical specifications		
Operating voltage	U _B	10 ... 30 V DC , class 2
Ripple		10 %
No-load supply current	I ₀	≤ 15 mA
Input		
Control input		light on +UB dark on: 0 V
Output		
Switching type		light/dark on electrically switchable
Signal output		1 PNP output, short-circuit protected, reverse polarity protected, open collector
Switching voltage		max. 30 V DC
Switching current		max. 100 mA , resistive load
Voltage drop	U _d	≤ 2 V
Switching frequency	f	≤ 1000 Hz
Response time		0.5 ms

Figure 69 Tachometer OBR2500-12GM40-E5-V1 technical data